STUDY OF COPPER ELECTRODEPOSITION ON RUTHENIUM OXIDE SURFACES AND BIMETALLIC CORROSION OF COPPER/RUTHENIUM IN GALLIC ACID SOLUTION

Kyle K. Yu, B.E.

Thesis Prepared for the Degree of

MASTER OF SCIENCE

UNIVERSITY OF NORTH TEXAS

August 2007

APPROVED:

Oliver M. R. Chyan, Major Professor
Teresa D. Golden, Committee Member
Michael G. Richmond, Chair of the Department of Chemistry
Sandra L. Terrell, Dean of the Robert B. Toulouse School of Graduate Studies

Yu, Kyle K. Study of Copper Electrodeposition on Ruthenium Oxide Surfaces and Bimetallic Corrosion of Copper/Ruthenium in Gallic Acid Solution, Master of Science (Analytical Chemistry), August 2007, 47 pp., 27 figures, reference list, 26 references.

Ruthenium, proposed as a new candidate of diffusion barrier, has three different kinds of oxides, which are native oxide, electrochemical reversible oxide and electrochemical irreversible oxide. Native oxide was formed by naturally exposed to air. Electrochemical reversible oxide was formed at lower anodic potential region, and irreversible oxides were formed at higher anodic potential region. In this study, we were focusing on the effect of copper electrodeposition on each type of oxides. From decreased charge of anodic stripping peaks and underpotential deposition (UPD) waves in cyclic voltammetry (CV), efficiency of Cu deposition dropped off indicating that interfacial binding strength between Cu and Ru oxides was weakened when the Ru surface was covered with irreversible oxide and native oxide. Also, Cu UPD was hindered by both O_2 and H_2 plasma modified Ru surfaces because the binding strength between Cu and Ru was weakened by O_2 and H_2 plasma treatment.

Cu/Ru and Cu/Ta bimetallic corrosion was studied for understanding the corrosion behavior between diffusion barrier (Ta and Ru) and Cu interconnects under the post chemical mechanical planarization (CMP) process in semiconductor fabrication. Gallic acid is used in post CMP slurry solution and is known well as antioxidant which is supposed to oxidize itself to prevent other species from oxidizing. However, in this study under the observation of Cu microdot corrosion test, copper was corroded only in gallic acid at specific pH region of alkaline condition which is close to the pH region for post CMP solution formula. With different pH alkaline condition, gallic acid formed different oxidized products which are characterized by cyclic voltammetry and UV-Vis spectroscopy. Therefore, the specific oxidized product from

particular pH region condition caused the Cu corrosion. Also, the corrosion rate of Cu microdots was influenced by substrate effect (Cu/Ru and Cu/Ta) and ambient control, which was included in this study.

ACKNOWLEDGEMENTS

I wish to express my gratitude to those who have encouraged and supported me to complete this dissertation.

I greatly appreciate my graduate advisor Dr. Oliver M. R. Chyan for his valuable advice, objective critiques and helpful suggestions. With his teaching and guiding hand, I learned knowledge of how to do and experience in doing it in both of my academic and personal life. The comments and critiques from Dr. Teresa Golden, my committee member, have greatly helped in making this dissertation a better shape. The financial support form the Welch Foundation, UNT Faculty Research Fund and Texas Instruments is deeply appreciated.

This work owes much to the thoughtful and helpful comments of my comrade-in-arms, Shyam S. Venkartaraman who is always willing to lend a hand, an idea, an ear or a tongue. Without his help, I can not image how tricky of my research life would be. I am indebted to a number of my present and past colleagues, Karthik S. Pillai, Fan Yang Dr. Tiruchirapalli Arunagiri, Dr. Yibin Zhang, Dr. Praveen Reddy, Oscar Ojeda, and Sarah Flores who have made this research group a gratification to work with.

I would like to thank my parents and parents-in-low for their unwavering support and confidence in my education. I would like to specially thank my wife, Tai-Fen Lee, for her encouragement and love. I can concentrate on my research.

Lastly I would like to thank DCC members and our pastor, Peter. With their concern and love, I became a Christian and understood that God is always guiding above us.

TABLE OF CONTENTS

Page

LIST OF FIGURES

CHAPTER 1

INTRODUCTION

This chapter will give brief introduction of instruments and techniques which are used in later chapters. Two studies are contented in this thesis. One of them is a study about the effect of ruthenium (Ru) native oxide on copper deposition which is described in chapter 2. The other one is a study about the effect of gallic acid on Cu/Ru bimetallic corrosion which will be discussed in chapter 3.

1.1 Fundamentals of Electrochemistry

The science of electrochemistry has been initiated since a shrinking muscle from frog dissection during anatomic experiment in the end of eighteenth century. Couple years later, a battery was developed by Alessandro Volta, and then Michael Faraday made electrochemistry become well developed in middle nineteenth century.[1] After that, lots of applications of electrochemistry have been explored and extended into our day to day life. Electrochemistry can be generally defined as the study of charge- or electron-transfer phenomena. In the electrochemistry, it contents a broad range of different physical and chemical field which includes coulometry, ion-selective electrodes, photosynthesis, and biochemistry etc. In addition, a lot of useful applications in electroanalytical measurements have been reported.[2,3]

1.1.1 The Nature of Electrochemical System[4]

There are some basic and important concepts about electrochemical systems. First, instead of homogeneous, the electrochemical system is usually heterogeneous because of the

electrode/electrolyte interface. For example, there are various electrode reactions taking place in heterogeneous condition, such as hydrogen evolution, copper plating, electrode oxidation and reduction. The solution of electrolyte can be separated in three parts which are double layer, diffusion layer and bulk layer shown in figure 1-1. The double layer is located within the interface between electrode interior and electrolyte and further is bulk layer. Second, surface reactions near the electrode usually cover several complicated kinetic steps which come with adsorption or deposition of atoms, intermediate products, migration of atoms, and recombination of atoms. Therefore, electrochemical systems show a dynamic nature that link with chemical transportation. Third, the current represents the reaction rate and the potential reflects the energy of electrons. Finally, potential and current are parameters which are inter-related to each other; as a result, two of them cannot be controlled in the same time.

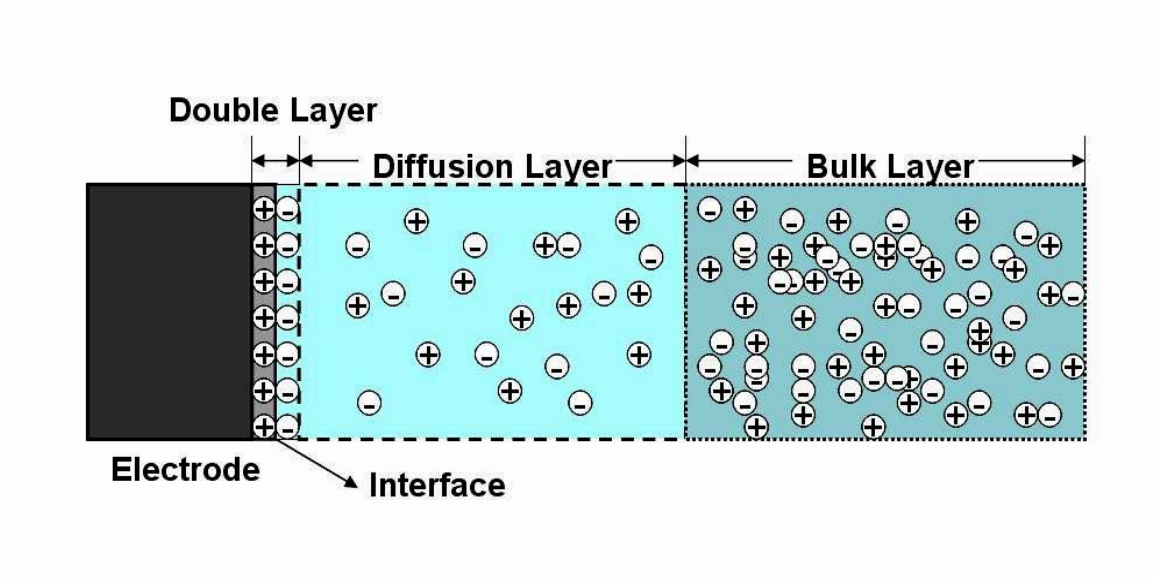

Figure 1-1: Configuration of layers of electrolyte in electrochemical system

1.1.2 Three Electrode System

Due to the advantage of precise electrode potential control during the measurement, the three-electrode method is the most widely used in electrochemistry. A reference electrode,

working electrode, and counter electrode (secondary or auxiliary electrode) are used in the system. An electrolyte is usually added to ensure satisfactory conductivity for charge transfer between electrodes. The range of the potential window is determined collectively by the mixture of the solvent, electrolyte and particular working electrode.

1.1.3 Open Circuit Potential

Open circuit potential (OCP) measurement is a fundamental property responding to the nature of working electrode in equilibrium with its chemical environments. The OCP value represents the stability of potential of working electrode in different ambients and can reflect the cleanliness of the electrode.

1.1.4 Cyclic Voltammetry

Cyclic voltammetry (CV) is one kind of potentiodynamic electrochemical measurement. The redox properties of chemicals in electrolyte or electrochemical reactivity of reactive electrode can be determined from CV. In CV, the potential is measured between the working electrode and the reference electrode and the current is recorded between the working electrode and the counter electrode. The CV experiment provides valuable information by plotting current (i) vs. potential (E). The potential is swept back and forth linearly with time in a pre-defined range. Take a reversible redox reaction as an example, the anodic forward scan will reach the potential of oxidation which produces the oxidative current peak, and the reverse scan will usually have a similar reduction current peak which has a symmetrical shape of oxidation peak. As a result, not only the potentials of each oxidation and reduction but also the rate of electrochemical reaction can be obtained. There is an example in figure 1-2. The redox reaction

of $Fe(CN)_6^{3-/4-}$ is represented as two current peaks which have peak current potentials of E_a and E_c.

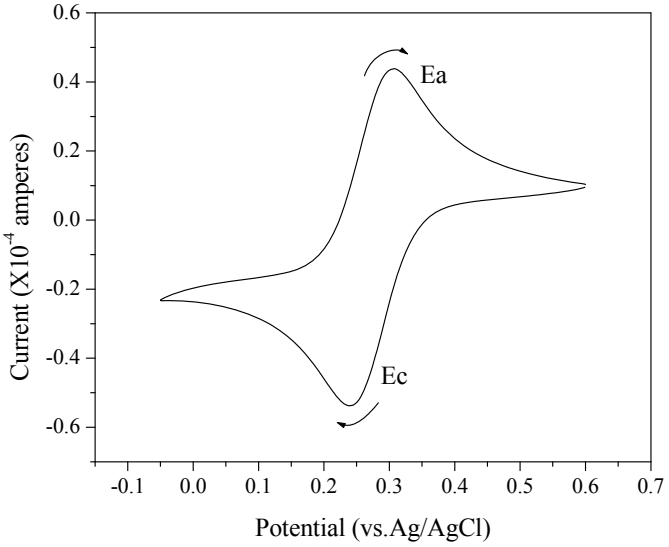

Figure 1-2: CV of redox reaction of Fe ion: 10mM $K_3Fe(CN)_6$ within 0.5M K_2SO_4 electrolyte scan rate: 50 mVs^{-1}

1.1.5 Tafel Plot[5]

Tafel plots relate to the tafel equation which concerns the rate of an electrochemical reaction to overpotential (η). Tafel plot is the graph of the logarithm of the current density (i) against the (η). A polarized electrode regularly produces a relationship between current and potential in a region which can be approached by:

$$\eta = \pm B \log (I/I_0)$$

Where η is applied overpotential with respect to the open circuit potential, I is the measured current density, B and I_0 are constants, I_0 is defined as the equilibrium current density, and B is defined as the Tafel Slope.

The Tafel plot is generated by starting the polarization at about -200mV from open circuit

potential (OCP) and increasing till the potential is +200mV from OCP. In figure 1-3, it shows that the corrosion current (I_{corr}) can be estimated by crossing extrapolation of cathodic and anodic current curves. The corrosion potential (E_{corr}) is allocated by extrapolation of the pointed tip of the tafel plot curve to the axis of potential V. This technique was used to measure the corrosion potential of Cu, Ta or Ru in gallic acid slurry solution.

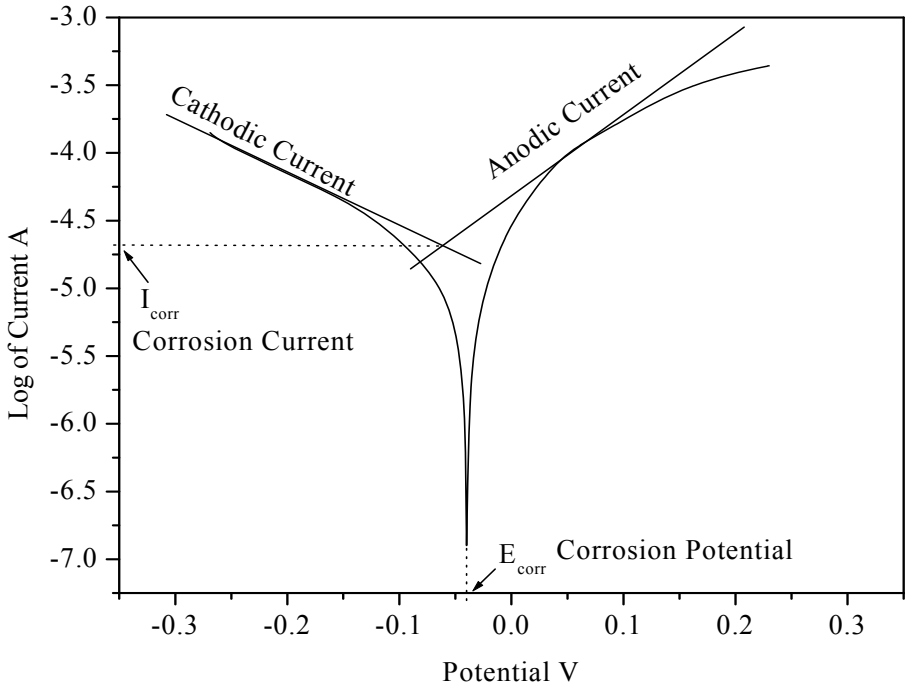

Figure 1-3: A typical Tafel plot of Cu electrode shows E_{corr}, I_{corr}, cathodic curve, and anodic curve.

1.2 Preparation of Metal Shot Working Electrode

In a three electrode system, the working electrode is an expendable material because the surface of the working electrode usually needs to be polished. Besides that there are many conductive materials can be prepared as working electrode, so the skill of making electrode is quite useful in electrochemical experiment.

1.2.1 Making the Mold

In order to create a mold that can hold the epoxy for encapsulating electrode, Pipet tip ($4^1/_2$ inch length) is served as a starting material for mold. Use the vise to secure the pipet tip and then cut off the non-tapered end of the pipette by hacksaw. Hold the mold with the vise again, and use the 5/64-inch drill bit to drill a hole in the middle of the mold for copper wire to go through. Then the mold is done.

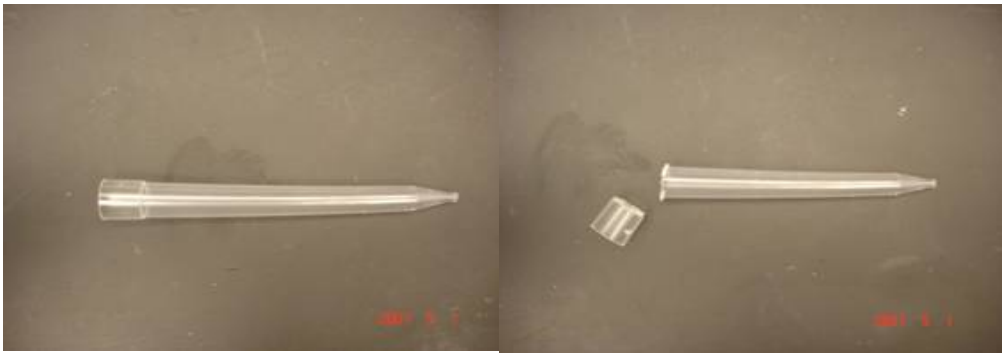

Figure 1-4: Making the mold

1.2.2 Making the Electrode

Cut a 6-inch piece of copper wire by using the wire cutters, and strip the cover on both ends of the wire. Place your metal disc on a clean and hard surface. Use the soldering gun to heat the disc and the copper wire and then solder them together. Place the mold on a sheet of parafilm with the larger uncut opening facing down, and put the shot inside the center of the mold. Make sure the copper wire goes through the drilled hole.

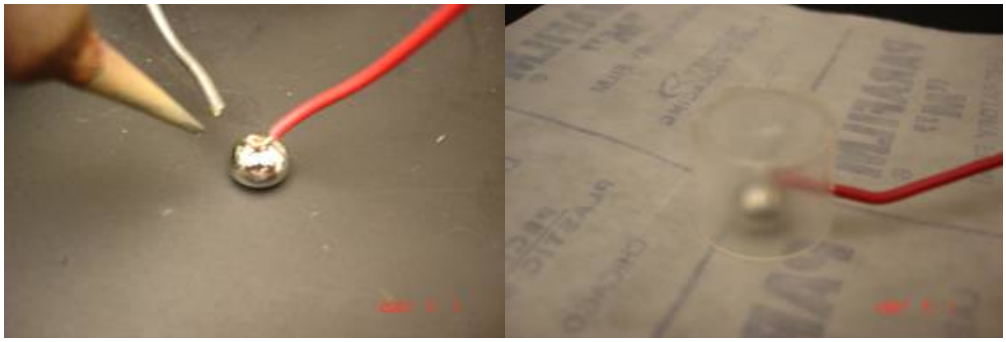

Figure 1-5: Soldering Cu wire and Ru disc then placing disc in the center of the mold

Prepare the Leco® metallographic epoxy liquid (Leco Corporation, Joseph, MI, http://www.leco.org/index1.htm) epoxy resin (LC) which is made by mixing resin and hardener. The weight ratio of resin and hardener is 100 to 14. Pour the epoxy slowly into the mold to prevent from forming bubbles and place it to cure at least 24 hours under a box enclosure. This will minimize the disturbance from room air currents. After the epoxy has dried and hardened, remove the plastic mold by making little cuts on the plastic mold with the wire cutters. The plastic mold should fracture into pieces, making the removal of the plastic mold relatively easy. At this step you already have an unpolished metal shot electrode encapsulated with epoxy.

1.2.3 Polishing the Electrode

Use the Enco® (Enco, Fernley, NV, http://www.use-enco.com/CGI/INSRHM) variable speed mini lathe instrument to cut the end of the electrode to make it flat for placing the stainless steel puck on the heat plate, and heat it for 5 minutes. Apply a thin layer of clear hot mounting wax from ALLIED® (Allied High Tech Products, Inc., Rancho Dominguez, CA, http://www.alliedhightech.com/index.html) on the surface of the steel puck, and place the unpolished electrode with the flat backside on the wax. Let it cool to allow the electrode to fix on puck well. Insert the steel puck with the unpolished electrode into the polishing holder or lapping

fixture. Loosen the side screw on the lapping fixture in order to adjust and select the amount that will be polished off.

Figure 1-6: Preparation of coarse grinding

For the coarse grinding, we polish the electrode surface with different grit size of silicon carbide (SiC). The grit size pad is used from 60, 180, 320, and 600 to 800. After coarse grinding, heat the stainless steel puck to melt the wax and remove the electrode from the puck. The fine grinding is to polish the surface from 6-micron (μ), 3μ and 1μ to 0.5μ grit diamond pad. At the end the surface will be mirror finished. Then the working electrode is ready for electrochemical experiments.

Figure 1-7: Coarse and fine grinding

1.3 Plasma Treatment

In the context of physics and chemistry, plasma is typically an ionized gas, and is different states of matter contrast to gases because the plasma has its unique properties. The meaning of ionized gas is that at least one electron has been dissociated from, or added to, a gas atom or molecule. So, plasma system contains electric charges of gaseous atoms or molecules

which have electrical conductivity. The main purpose of plasma processing is to modify the properties of a surface. The processes include plasma activation, plasma modification, plasma polymerization, and plasma surface interactions. Plasma activation is another name for plasma functionalization. Surface is usually activated by plasma to improve adhesion properties for coating, painting, etc. In this study, the ruthenium surface was activated by different gas plasma. Weakly ionized oxygen plasma was used to oxidize the Ru surface, whereas the surface was reduced by applying ionized hydrogen plasma. The plasma treatment for oxidizing and reducing surface was used to compare with the electrochemical treatment of oxidized and reduced surface in chapter 2.

1.4 UV-Visible Spectroscopy[3,6]

UV-visible spectroscopy (UV-vis) is the measurement of the wavelength and intensity of absorption of analyte. Tungsten lamp is light source in visible light region (wavelength from 240-2500nm) and D_2 lamp is used in ultraviolet (UV) region (wavelength from 160-380nm). Ultraviolet and visible light are energetic enough to promote outer electrons to higher energy levels. Even though UV-vis has limitation for chemical identification, its spectra are very useful for quantitative measurements. UV-vis is generally used in the quantitative determination of molecules and inorganic ions or transition metal ion complexes in solution. It is necessary to know how quickly the absorbance changes with concentration. The absorbance of a solution is directly proportional to the concentration of an analyte in solution at specific wavelength (is often represented by the symbol λ) according to the Beer-Lambert Law. In the region of relatively small concentrations absorbance follows Beer-Lambert law:

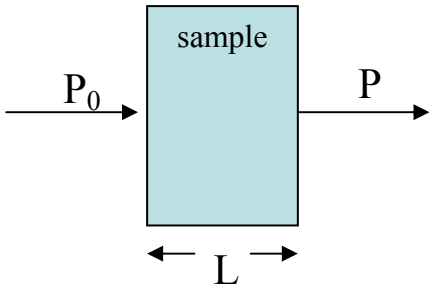

$$A = \log (P_0/P) = \varepsilon \times c \times L$$

where A is the measured absorbance, P_0 is the intensity of the incident light at a given wavelength, P is the transmitted intensity, P_0 / P is called the transmittance, L is the light path in the cuvette, and c the concentration of the substance, ε is molar absorption coefficient.

Most samples for UV/Vis are liquids, even though the absorbance of gases and even of solids can also be measured. Samples are usually placed in a transparent cell, known as a cuvette which are commonly rectangular shape with an internal width of 1 cm. (This width becomes the path length, L, in the Beer-Lambert law.)

The UV-Vis spectroscopy was used in chapter 3 for explaining the complexation behavior of copper ion and gallic acid, and showing absorbance of the quinone from gallic acid.

1.5 References

1. Rieger, Philip H. *Electrochemistry*; Chapman & Hall: New York, 1994; Chapter 1. p 3.
2. *Laboratory Techniques in Electroanalytical Chemistry,* 2nd ed., rev. and expanded,; Kissinger, Peter T. Ed.; Heineman, William R.Ed.; Marcel Dekker, Inc.: New York, 1996; Chapter 2.
3. Skoog; West; Holler; *Fundamentals of analytical chemistry*, Eighth ed.; Thomson: Belmont, 2002; Chapter 1, p 25.
4. Faulkner, Larry R. *Journal of Chemical Education*. **1983,** 60(4), 262.

5. Trethewey, Kenneth R. Corrosion for student of science and engineering, Longman Scientific & Technical: New York, 1988; Chapter 4. pp 82-86.

6. Rao, C. N. R. *Ultra-violet and Visible spectroscopy*: Chemical applications, Plenum press, 1967.

CHAPTER 2

THE EFFECT OF RUTHENIUM OXIDE ON COPPER ELECTRODEPOSTION

2.1 Introduction

In the industry, Ta/TaN or TiN/Ti has been used as bilayer barrier films for copper diffusion barriers.[1-4] The Tantalum cannot bind well on SiO_2 and so the TaN is used as an adhesion layer. Recently, the size of integrated circuit (IC) is being shrinked in the industry to follow Moore's law which means doubling transistors in IC chip every eighteenth months.[5] Due to the difficulty of scaling Ta/TaN bilayer as copper barrier films, research is in process for finding new candidates of diffusion barrier with only one layer. In Pt group, ruthenium is one of the candidates for copper barrier because of the properties such as high thermal and chemical stabilities, high electrical conductivities, and high melting point and less solubility of Cu on Ru even at high temperatures. Also, electrochemical Cu underpotential deposition (UPD) on Ru which demonstrates the strong interfacial binding between Ru and Cu plays a significant role in Cu-plating diffusion barrier performance.[6] Presently, there has been increasing interest in studying Ru as barrier material because the ultra thin Ru can be used as barrier without copper seed layer.[7,8] However, the effect of different treatments of Ru surface as the substrate for Cu deposition becomes increasingly more important. This chapter describe the study of Cu electrodeposition on different treated Ru surface such as air exposed Ru surfaces (growing thick native oxide), fresh polished Ru surface, electro-oxidized and reduced Ru surface, hydrogen- and oxygen-plasma etching treatment. From this chapter, the characteristics of Ru surface and its influences on Cu plating were systematically studied.

2.2 Material Preparation and Experimentation

ESPI Ru shots (Electronic Space Products International, Ashland, OR, http://www.espi-metals.com/) shots were made into disks working electrodes, the details of electrode fabrication is described in Chapter 1. Before the experiment, the final surface of Ru shot was mirror polished by different grit size of silicon carbide (SiC) pads from Allied Hi-Tech (Allied High Tech Products, Inc., Rancho Dominguez, CA, http://www.alliedhightech.com/polishing/). The geometric area of the Ru electrode is ca. 0.34cm^2. A Pt sheet is used as the counter electrode. A saturated silver/silver chloride, reference electrode (Ag/AgCl 0.197V Vs. SHE), is used as the reference electrode. All potential values are referred against Ag/AgCl in this chapter. The three electrode electrochemical cell set up was used for voltammetric measurements which were performed by using 440a and 760b series model electrochemical analyzer from CHI (CHI instruments, Inc, Austin, TX, http://www.ijcambria.com/TREQCM.htm). In order to prepare 0.5M sulfuric acid with 2mM copper sulfate electrolyte solution as plating bath for Cu to deposit on Ru, high purity (99.999%) copper sulfate pentahydrate from Aldrich® (Sigma-Aldrich Co., Milwaukee, WI, http://www.sigmaaldrich.com/) and 96.2 weight % sulfuric acid from Mallinckrodt Baker, Inc. (Mallinckrodt Baker, Inc. Phillipsburg, NJ, http://www.biospace.com/company_profile.aspx?CompanyID=558520) were used.

Extra pure research grade hydrogen gas comes from AIR LIQUIDE (AIR LIQUIDE AMERICA, Suite 1800 Houston, TX, http://www.airliquide.com/home.html). The purity of hydrogen gas is 99.9995%. The hydrogen gas is used as feeding gas resource in plasma system or pre-conditioning electrolyte in electrochemical analysis for CHI instruments, Inc. Electrochemical reduction or oxidation of the working electrode can be achieved by applying negative or positive potentials respectively. For example, surface of the working electrode can be reduced by applying cathodic potential at -0.4V in 0.5M sulfuric acid. Similarly, the Ru surface

can also be oxidized by applying anodic potential at 1.3V in 0.5M sulfuric acid. Besides electrochemical reduction and oxidation, the Ru surface can be cleaned by using the plasma cleaner from HARRICK PLASMA (HARRICK PLASMA, Ithaca, NY, http://www.harrickplasma.com/). Plasma cleaning is a dry process for surface treatment whereas electrochemical reduction is a wet process. The surface is activated by plasma treatment with different gas sources such as hydrogen (reducing), oxygen (oxidizing), argon (cleaning), ammonia (cleaning) or mixed gases.

2.3 Ruthenium Native Oxide

Ruthenium native oxide is formed naturally when the surface is exposed to air.[9,10] The thin layer of native oxide is formed rapidly even on a freshly polished Ru electrode surface. Therefore, the difference of Cu deposition on reduced Ru surface and surface with native oxide layer becomes a fundamental issue for Ru as the barrier material. Subsequently, experiments of OCP (open circuit potential) and CV (cyclic voltammogram) are carried out to examine the formation of Ru native oxide.

2.3.1 Oxidation and Reduction of Native Oxide on Ru

Cyclic voltammetry is a very useful technique in electrochemistry, which is described in chapter 1 in detail. Figure 2-1, shows first two CVs of 24 hours air-exposed Ru shot in 0.5 M sulfuric acid. No prepurging gas was used and solution was exposed to the lab ambient. The open-circuit potential (OCP) of the native oxide is 0.52V~ 0.55V. Solid line is the first scan of CV which shows a reduced wave in cathodic region around -0.15V, but the reduced wave doesn't show in the second CV, which means the Ru surface was electrochemically reduced after the first

scan.

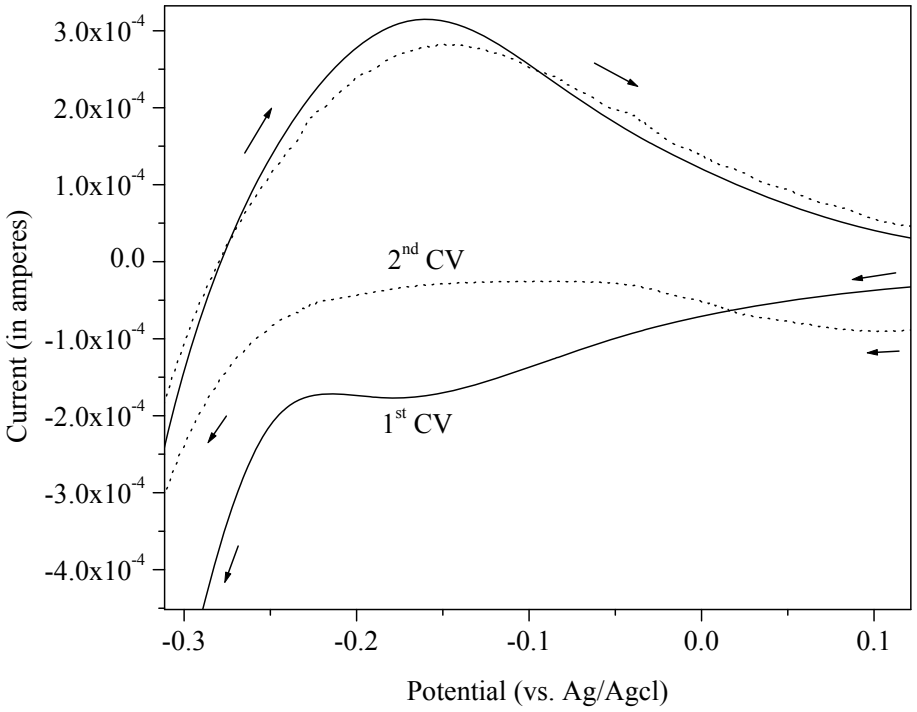

Figure 2-1: Cyclic voltammograms of 24 hr air-exposed Ru in 0.5 M H_2SO_4 at a scan rate of 50mV/s. The native oxide reduction wave is centered ca. -0.15 V vs. Ag/AgCl. Solid line represents the first CV and dotted line represents the second CV. Absence of native oxide reduction wave can be clearly seen in the second CV.

The effect of different ambients on Ru native oxide formation was studied in hydrogen and nitrogen environments. The background solution was purged by nitrogen and hydrogen to decrease the solubility of oxygen in solution for 15 minutes; N_2 or H_2 blankets was then maintained over the solution during the CV. In the figure 2-2, comparing two purged ambients, the native oxide reduction peak around -0.15V is completely absent in hydrogen ambient, thus reflecting hydrogen as a better reducing gas for reductive removal of Ru native oxide.

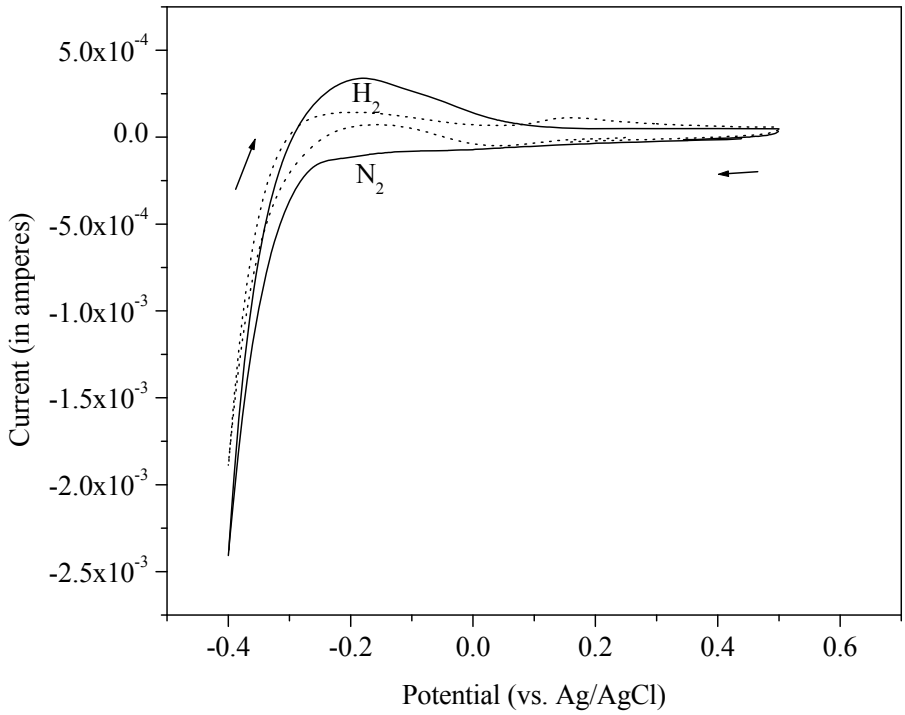

Figure 2-2: First CV of freshly polished Ru in 0.5M H_2SO_4 in N_2 (solid) and H_2 (dotted) environments at a scan rate of 50mV/s. Native oxide reduction wave is absent in H_2 environment.

2.3.2 Open-Circuit Potential of Ru in Different Ambients

As seen above, with no applied potential prior to CV, native oxide gets reduced in H_2 ambient. To investigate more on the effect of different ambients, OCP measurements were carried out. OCP of polished Ru surface in nitrogen and hydrogen pre-purged H_2SO_4 was around 0.45V and –0.29V respectively in the figure 2-3. The OCP of freshly polished Ru surface in hydrogen environment decreases from 0.35V to 0.1V and then rapidly goes down to a steady potential around -0.29V. The negative OCP value (-0.29V) of Ru shot is observed in H_2 pre-purged environment likely due to the reaction of proton/hydrogen exchange interaction with the surface.

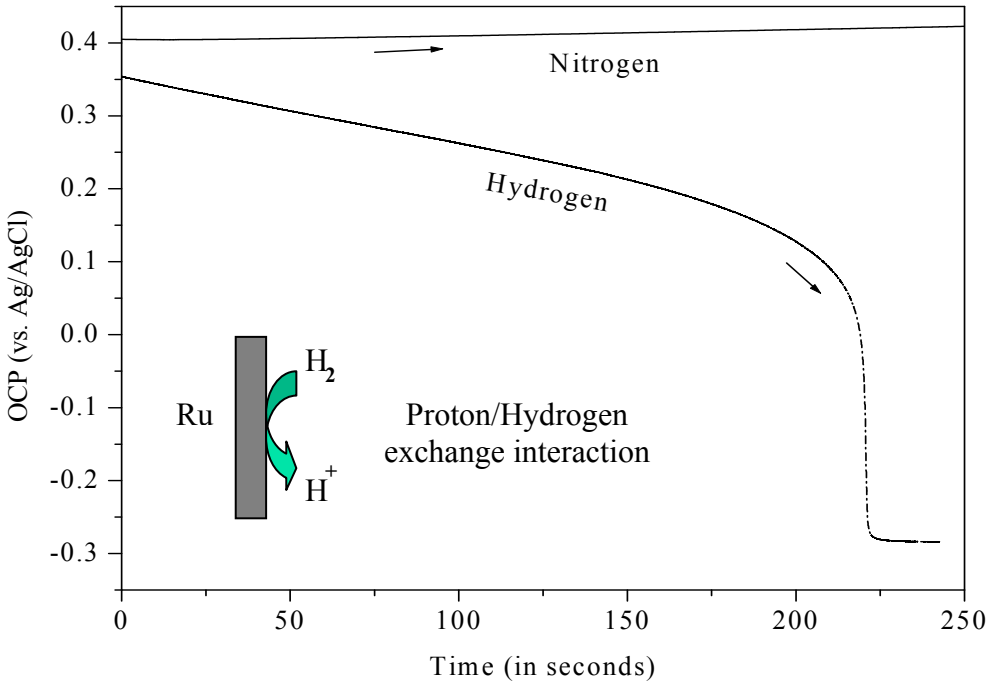

Figure 2-3: OCP of freshly polished Ru in H_2 purged 0.5M H_2SO_4 solution. Ru reached steady state potential of -0.29V in H_2 environment wherein the potential value is attributed to the reversible proton/hydrogen reaction.

In separated experiments both platinum and palladium have the similar OCP values like Ru in Hydrogen environment. In Figure 2-4, OCP measurements of fleshly polished Ru, Pd, and Pt electrodes immersed in the same volume of 0.5 M sulfuric acid which was purged with hydrogen for 15 minutes are shown from these three OCP values, the OCP of Pt and Pd drops faster rather than Ru. Also, all of the OCP values eventually stabilized at a negative potential around -0.29V and lasted for more than one hour with blanket hydrogen around the cell.

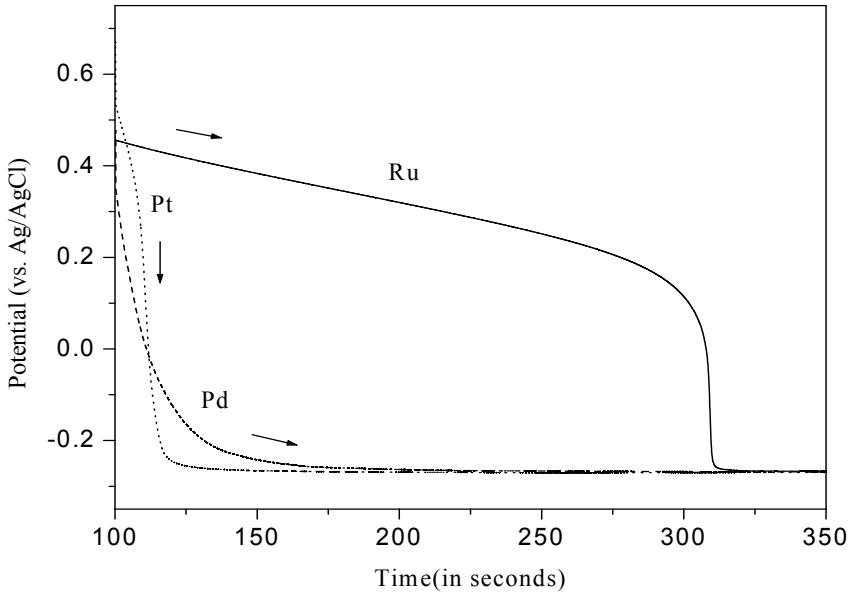

Figure 2-4: OCP of freshly polished Ru, Pd and Pt in H_2 purged 0.5M H_2SO_4 solution

Previous OCP data in figure 2-3 shows that the OCP value goes to stable potential at (-0.29V) in H_2 environment. The OCP of Ru is continual decreasing and eventually cross the native oxide reduction potential -0.15V (figure 2-3) indicates purging hydrogen gas into the solution reduces Ru native oxide from its surface. It is important to note that the surface can be free of oxide in hydrogen ambient control. Pre-conditioning of purging N_2 or H_2 in 0.5 M sulfuric acid for 15 minutes minimize the soluble oxygen in solution; as a result, the OCP value of Ru surface decreases due to the limited chance of oxygen contact the Ru surface thereby preventing the formation of native oxide. H_2 pre-purged environment not only inhibits the oxidation of Ru surface but also can reduce the native oxide layer on Ru surface.

2.3.3 The Effect of Ru Native Oxide on Cu Deposition

Since the Ru surface can be reduced by electrochemical reduction by holding the Ru

surface at negative potential to remove the native oxide on the surface[6], this allow us to quantitize the native oxide formation on Ru shot. In order to maintain the reproducible Ru surface, the Ru shot was polished once before the first air exposure experiment, then the air-exposed Ru shot was clean by electrochemical reduction (hold at -0.4V for 2 minutes) before each new air exposed run. After the air exposure, OCP value of air exposed Ru was measured and CV was recorded starting from OCP to -0.4V. In figure 2-5 shows CV of Ru native oxide on its surface. Exclude freshly polished Ru surface, the native oxide reduction peak grows with more exposure to air, which means that the coverage of Ru native oxide increases when the surface is exposed to air.

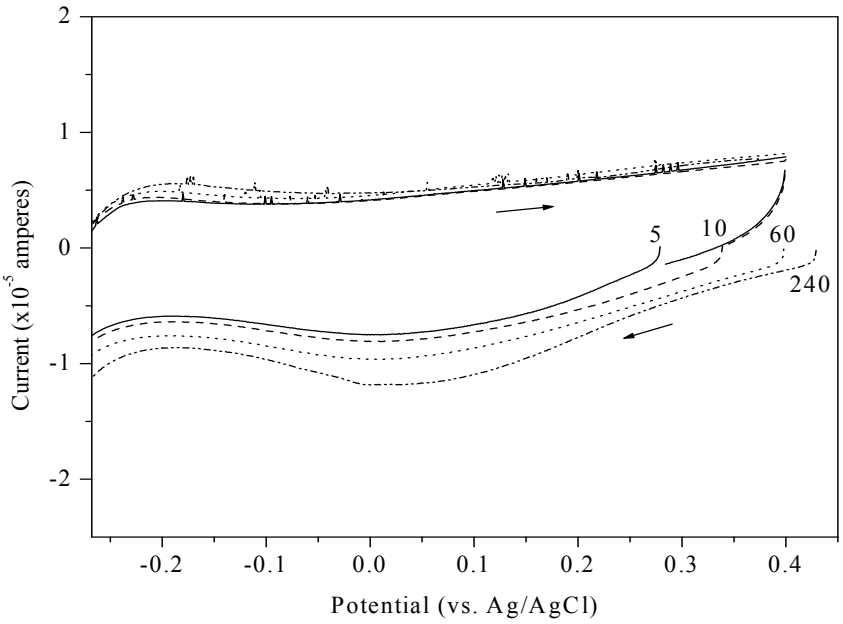

Figure 2-5: CVs of growing oxide by exposing to air in varying interval time (5-240 min) in 0.5M H_2SO_4

The CHI electrochemical analyzer instrument has the program to calculate the charge of current peak in cyclic voltammetry. Therefore, the stripping charge of each native oxide reduction peak shown in figure 2-6 was calculated. Both the charge of the peak and the OCP

value can represent the state of the Ru surface. From OCP data, the OCP value of saturated air exposure Ru native oxide is higher than the OCP value of electrochemical reduced surface. In the other words, the OCP value keeps increasing with the increase in native oxide layer thickness on the Ru surface. From figure 2-6, saturated native oxide coverage on Ru can be reached within a time period of 180 minutes (3 hours).

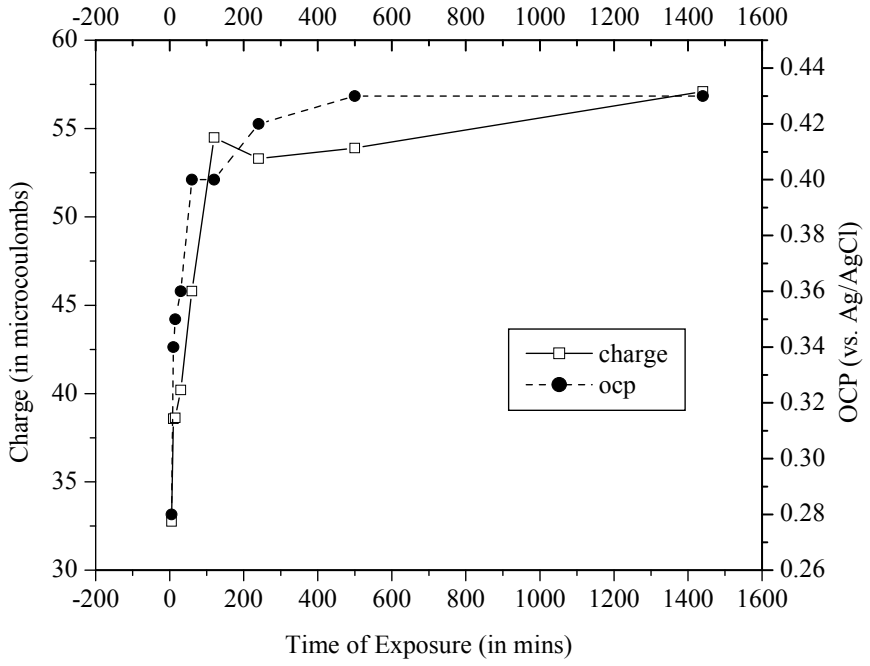

Figure 2-6: The stripping charge of native oxide reduction and OCP value vs. time of exposure

2.4 The Effect of Ru Surface Conditions on Cu Electrodeposition

Following the previous study on Ru native oxide, we explore the effect of Ru surface on Cu electrodeposition. The work is crucial since the native oxide will dominate the Ru/Cu interface before plating thin layer of Cu. Following is the experiment to investigate Cu underpotential deposition (UPD) on different interval air-exposed Ru surfaces. Before the

experiment, the Ru disk shot (working electrode) is polished completely by fine size pad (≤1μm). The flatness of Ru disk shot is very important in order to calculate the correct geometric served area of Ru surface. From the charge of UPD stripping area of Ru surface, monolayer coverage of Cu UPD on Ru can be determined by the formula,

$$Monolayer(ML) = \frac{QN_a}{nFA(10^{15})}$$

Where,

Q – Charge of Cu UPD stripping (in coulombs)

N_a – Avogadro number ($6.022X10^{23}$)

n – Number of the electrons for Cu^{2+} reduction = 2

F – Faraday constant (96500 Coulomb/mole)

A – Geometric area (cm^2)

2.4.1 The Effect of Native Oxide on Cu UPD

In figure 2-7, the CV clearly shows that the copper UPD striping peak around 0.15V from oxide-covered Ru electrode keeps decreasing when the air exposure is increasing. Due to the fact that the Ru native oxide grows when the surface is exposed to air, increases the coverage of oxygen atoms on the surface thereby leaving only a lesser amount of fresh surface for Cu deposition. In other words, the binding force between Cu atom and Ru native oxide surface is not strong as Cu atom and Ru surface. Hence, the native oxide layer decreases the efficiency of both bulk and UPD Cu plating on Ru surface.

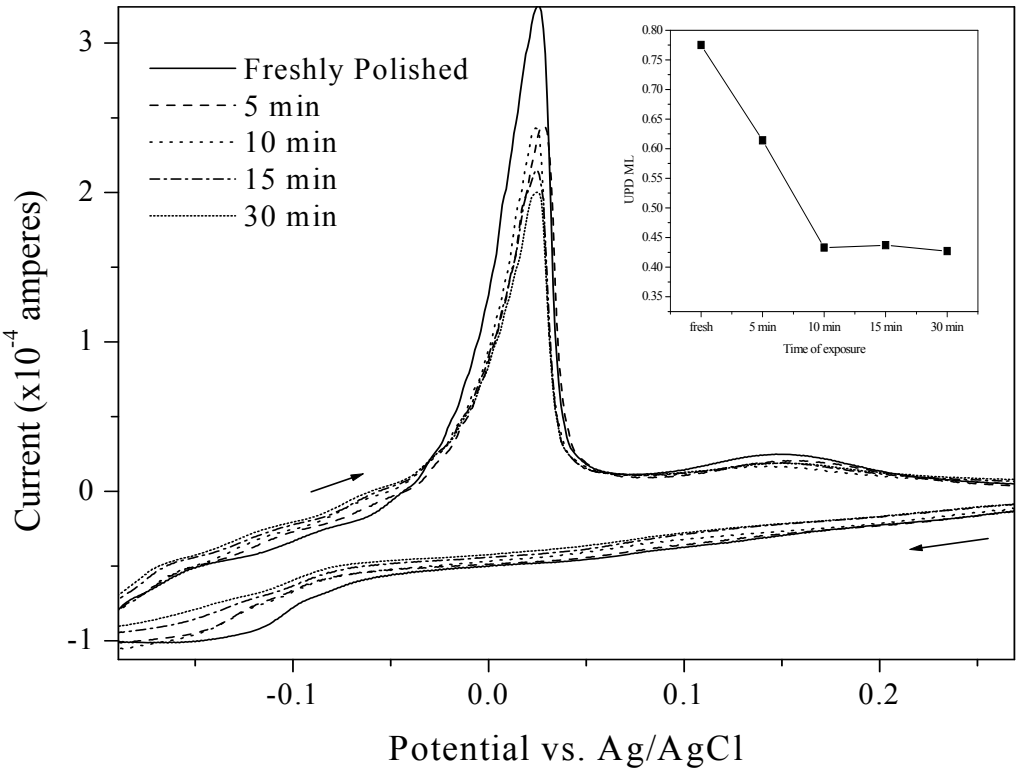

Figure 2-7: Cu electrodeposition on Ru surface immersed in 2mM $CuSO_4$/0.5M H_2SO_4 at a scan rate of 20 mV/s. *Insert:* Cu UPD Monolayer (ML) coverage on Ru at different time intervals of air exposure.

2.4.2 The Effect of Electrochemical Oxide on Cu UPD

Previously, the Ru native oxide was shown to hinder the Cu deposition. Also, it will be interesting to compare the cases of the native oxide with the electrochemical oxide formed on Ru surface. Electrochemical oxide can be formed by applying certain potential to oxidize surface of metal electrode.[11] It was previously demonstrated that Ru oxide (RuO_xH_y) formed at 1.3V and fresh polished Ru surface are conductive and have strong binding with Cu.[6,12,13] These two materials both have Cu UPD. Therefore, Ru oxide was made by holding different potentials (0.55V, 0.65V, 0.85V, 0.95V, 1.1V, 1.2V and 1.3V Vs. Ag/AgCl) for 30 seconds. Ru surface was polished freshly before electrochemical oxidizing Ru surface. In figure 2-8, first CV's of anodic

Cu stripping on different electrochemical Ru oxide surfaces are shown. Both the peak current and charge associated with Cu bulk stripping decreases when the Ru surface was oxidized from 0.55V to 1.10V. However, the peak current increases when Ru surface was oxidized over 1.10V.

Cu UPD measurements also show that the oxidized potential around 1.10V does change Ru surface to lose its attraction to the first Cu layer deposition on its surface. In figure 2-9, the Cu UPD peak of anodic CV shows that the each oxidized potentials have different behavior of Cu UPD. The Cu UPD peak coverage again reaches its minimum at the transition potential 1.10V. From the V shape curve of the inserts in both figures 2-8 and 2-9 point out that the electrochemical Ru oxide formed at around 1.10V is likely a transition sate between reversible oxides and conducting oxides (RuO_xH_y).

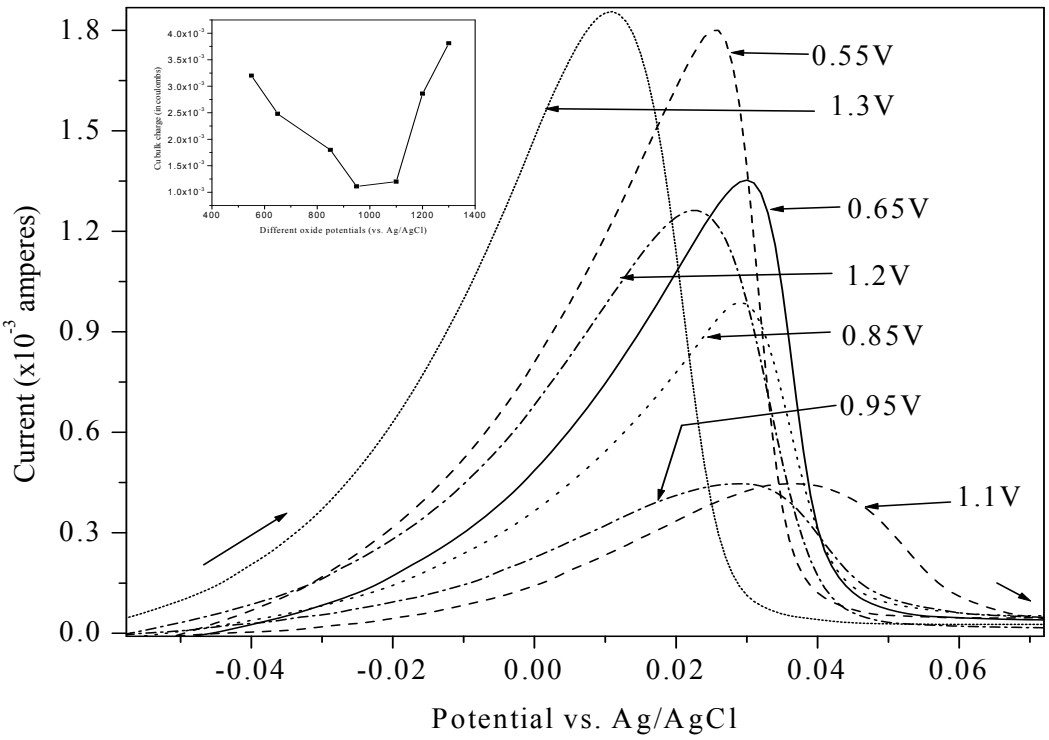

Figure 2-8: Anodic Cu bulk stripping on RuOx/Ru formed at various potentials as mentioned in the text and figure. *Insert*: Cu bulk charge vs. potential of RuOx/Ru. Oxide formed till 1.1 V affects Cu plating efficiency and > 1.2 V greatly improves the Cu plating characteristics.

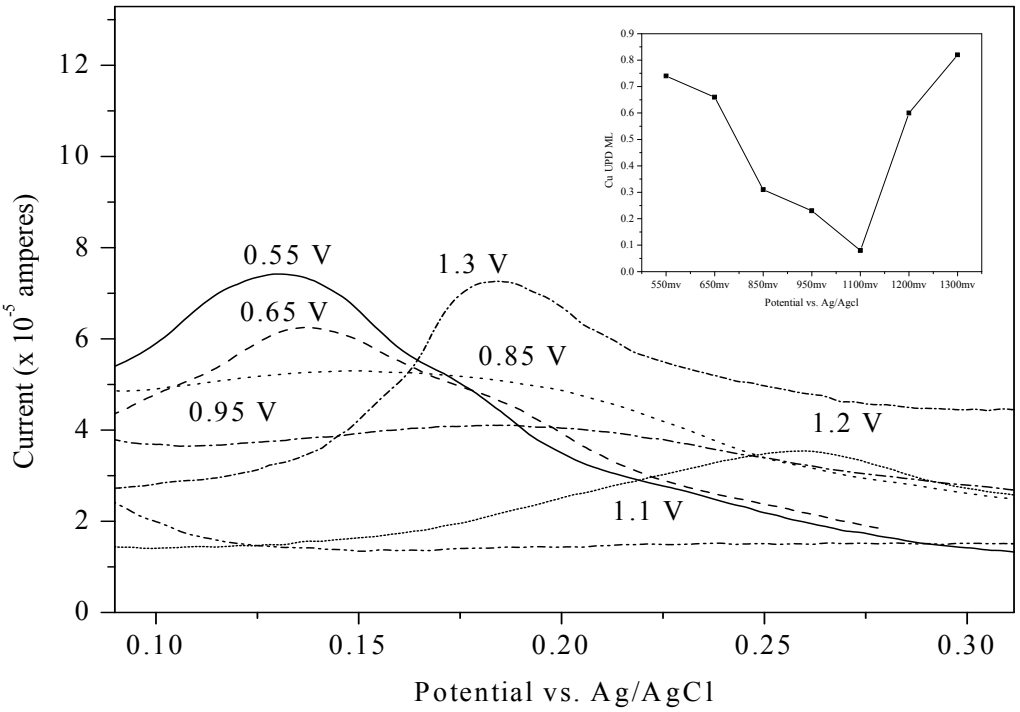

Figure 2-9: Cu UPD on RuOx/Ru formed at various positive potentials as mentioned in the text. *Insert*: Cu UPD ML on RuOx/Ru. Decrease in the ML within the reversible region suggests that interfacial binding is weak whereas it's strong for Cu UPD on irreversible RuOx/Ru.

From the stripping peak and Cu UPD peak in anodic CV, the charge of these peaks in each specific oxidized potentials are collected and be plotted in figure 2-8 and figure 2-9. The charge of the UPD wave can tell the number of Cu atoms plating on the Ru surface. In other words, the charge of the stripping peak presents the Cu plating efficiency. In figure 2-8, the Cu plating efficiency drops when the oxidized potential increases from freshly polished Ru surface 0.55V to 1.10V oxidized surface. Furthermore, in figure 2-9 (insert), from calculation of the charge of Cu UPD peak, the values of monolayer of Cu atoms on Ru surface shows that the monolayer decreases from 0.75 to less than 0.1 when the oxidized potential at 1.10V. Comparing with air-exposed Ru oxide, although the Ru native oxide seems to be saturated on Ru surface after exposed to air couple of hours, but the monolayer of Cu UPD doesn't drop as much as Ru

electrochemical oxide prepared at potential 1.10V. So, the potential around 1.10V can be the transition potential from reducible oxide to irreducible oxide.

2.5 Treatment of Ru Surface by Plasma Modification

Plasma treatment is a surface processing method in which a high flow of plasma is directed at a metal substrate. Plasma contains electrically charged particles, ions, neutral atoms and molecules. Plasma is generated by ionization of gas molecules when stroked by highly energetic electrons. The plasma can be generated using different gases like hydrogen, oxygen, nitrogen, ammonia etc., depending on the nature of treatment desired. For example hydrogen plasma can be generated to reduce the surface. Both hydrogen and ammonia plasma are widely used for cleaning high aspect ratio structure on semiconductor surface at low temperature. Similarly O_2 plasma can be used to oxidize the surface. Besides oxidizing metal surface, O_2 plasma is also used to etch away any organic residues on a metal surface. In this study the effect of hydrogen and O_2 plasma are compared by investigating Cu UPD on the plasma treated Ru surface. Before and after plasma treatment, the surface condition of Ru was determined using CV and OCP measurements.

2.5.1 Cu UPD on O_2 Plasma Treated Ru Surface

Purple colored O_2 plasma was generated by purging high purity O_2 gas inside the plasma chamber under a vacuum pressure of 100 mTorr and RF power of 30 watts. Compared to the other gases used like H_2 and N_2 (200 mTorr), O_2 plasma can only be generated at a higher vacuum condition.

To investigate the effect of O_2 plasma treatment on Cu UPD, three different surfaces of

Ru were compared: (i) 3 day exposed Ru (thick native oxide covered), (ii) freshly polished Ru and (iii) O_2 plasma treated Ru surfaces. Also to study the effect of O_2 plasma treatment, time dependent experiments were also done by plasma treating the Ru surface at 5 mins and 10 mins. Figure 2-10 shows the overlay of first CV of Cu UPD (highlight of 0.1-0.35V) on different Ru surface conditions. It can be clearly seen that 15 minutes O_2 plasma treatment completely hinders the deposition of Cu UPD on the Ru surface which is observed by the flat CV ca. 0.25 V. The same peak behavior was seen only in case of UPD on +1.1 V electrochemical oxide formed on Ru indicating the 15 minutes O_2 plasma treated surface is similar to the +1.1V electrochemical oxide.

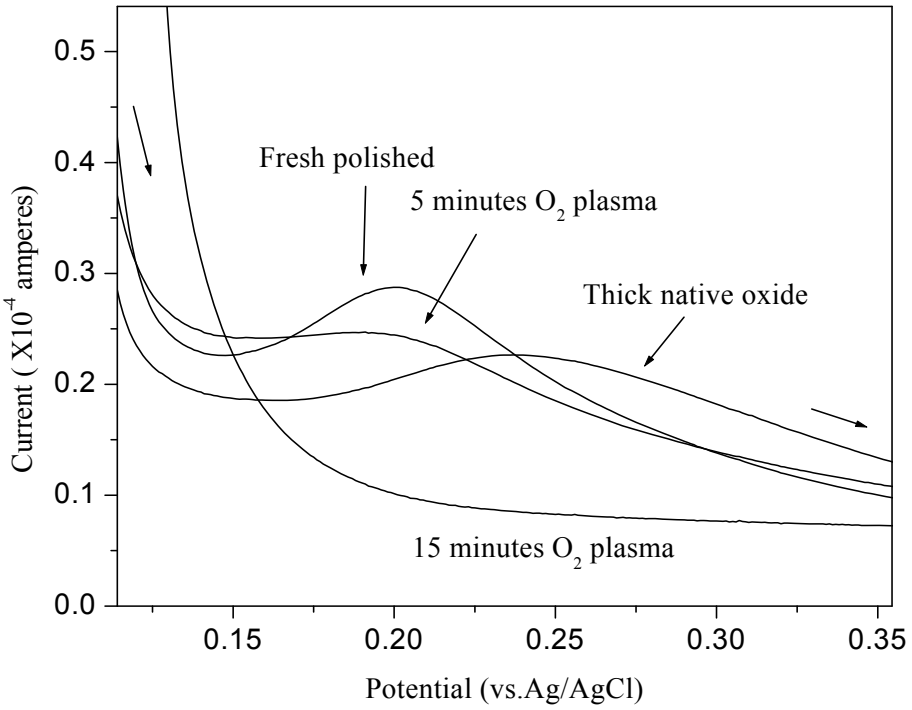

Figure 2-10: First CVs of Cu UPD on RuOx/Ru formed by air exposure and O_2 plasma modification in 2mM $CuSO_4$/0.5M H_2SO_4 solution

2.5.2 Cu UPD on H_2 Plasma Treated Ru Surface

Previously we have seen that purging hydrogen gas reduces the native oxide on Ru. Similar to it, H_2 plasma was also used for treating the Ru surface to investigate the Cu UPD behavior. In figure 2-11, the CV of thick native oxide wafer and the CV of 30 minutes H_2 plasma treated wafer in background (0.5M H_2SO_4). The reduction of native oxide (at -0.15V- -0.20V) was absent after H_2 plasma treatment. So, H_2 plasma can reduce the native oxide of Ru surface.

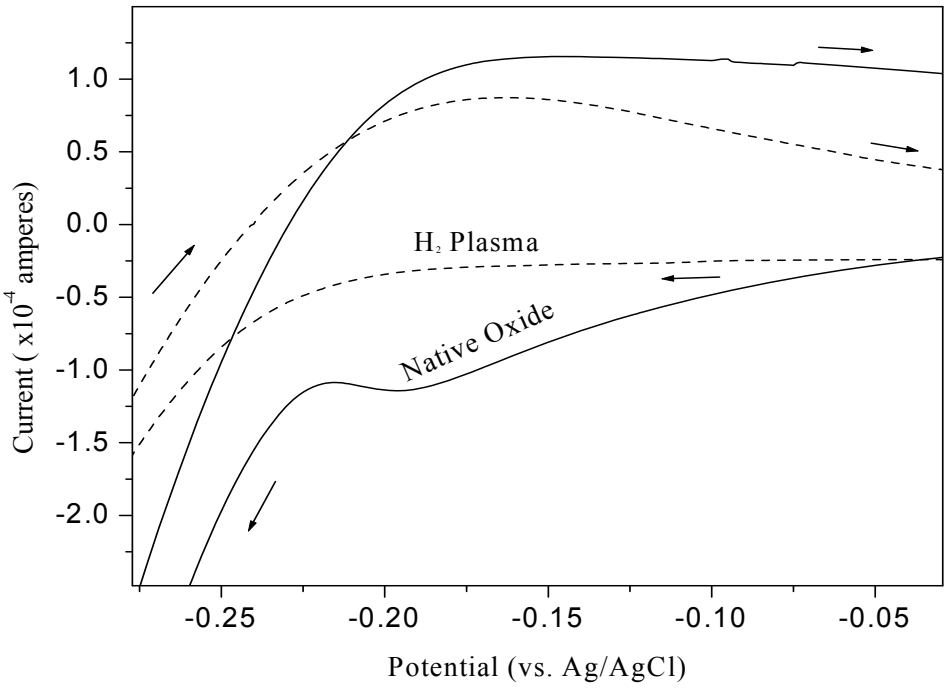

Figure 2-11: First CVs of Ru wafer in 0.5M H_2SO_4 at a scan rate of 20mV/s. Native oxide reduction wave is absent in H_2 plasma treated condition.

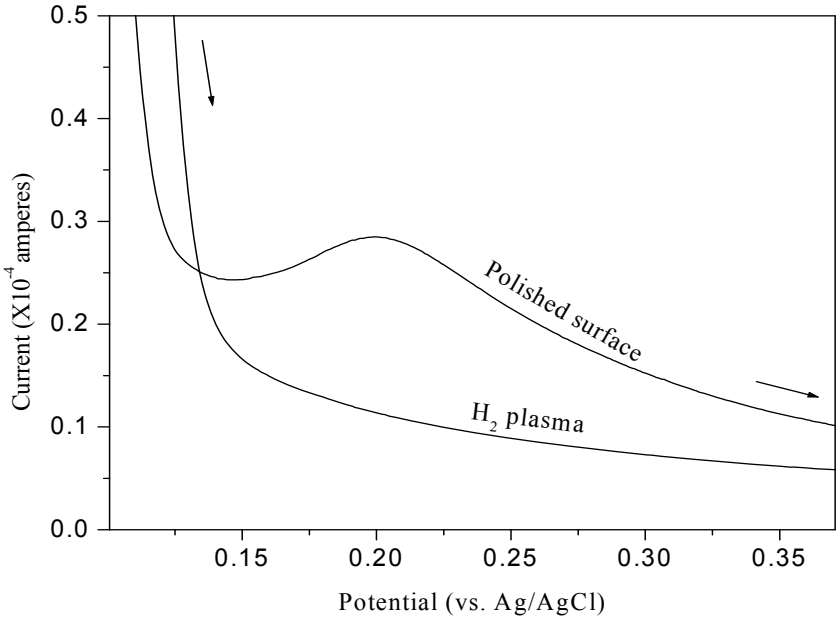

Figure 2-12: First CVs of Cu UPD on freshly polished Ru surface and H_2 plasma treated Ru surface in 2mM $CuSO_4$/0.5M H_2SO_4 solution.

However, the CV of Cu UPD on H_2 plasma treated Ru surface didn't show UPD wave that is opposite to the expectation, shown in figure 2-12. The H_2 plasma treatment not only reduced the surface but also passivated the surface making the surface platform unfavorable for Cu UPD. Further investigation is needed to explore this interesting observation.

2.6 Conclusions

The growth of Ru native oxide upon air exposure does diminish the efficiency of Cu UPD, ML and bulk plating on Ru surface. Saturated native oxide can be formed in air-exposed ambient after three hours. Second, the native oxide can be removed by hydrogen pre-purged condition or electrochemical reduction. Third, electrochemical formed oxide can be reversible when applied potential is less than 1.10V, but it changes to irreversible oxide (RuO_xH_y) when

applied potential is greater than 1.20V. Finally, the oxide can be recovered when the OCP treated-Ru surface is less than 0.70V. However, it becomes irreversible oxide after 15 minutes of oxygen plasma treatment because the OCP value becomes more that 0.70V.

2.7 References

1. Olowolafe, J. O.; Mogab, C. J.; Gregory, M. Kottke. *J. Appl. Phys.* **1992**, 72(9),
2. Wang, M. T.; Lin, Y. C.; Chen, M. C. *J. Electrochem. Soc.***1998**, 145, 7.
3. Holloway, Karen; Fryer, Peter M. *Appl. Phys. Lett.* **1990**, 57(17), 22.
4. Ono, H.; Nakano, T.; Ohta, T. *Appl. Phys. Lett.* **1994**, 64(12), 21.
5. Schaller, R. R.: *Spectrum, IEEE*. **1997**, 34(6), 52-59.
6. Zhang, Yibin; Huang, Long; Arunagiri, Tiruchirapalli N.; Ojeda, Oscar; Flores, Sarah; Chyan, Oliver; Wallace, Robert M. *Electrochemical and Solid-State Letters.* **2004**, 7(9), C107-C110.
7. Josell, D.; Wheeler, D.; Witt, C.; Moffat, T. P. *Electrochemical and Solid-State Letters*. **2003**, 6(10), C143-145.
8. Chan, R.; Arunagiri, T. N.; Zhang, Y., Chyan, O.; Wallace, R. M.; Kim, M. J.; Hurd, T. Q. *Electrochemical and Solid-State Letters.* **2004**, 7(8), G154-157.
9. Moffat, T. P.; Walker, M.; Chen, P. J.; Bonevich, J. E; Egelhoff, W. F.; Richter, L.; Witt, C.; Aaltonen, T.; Ritala, M.; Leskela, M.; Josell, D.; *J. Electrochem. Soc.* **2006**, 153(1), C37-C50.
10. Liu, J.; Lei, J.; Magtoto, N.; Rudenja, S.; Garza, M.; Kelber, J. A. *J. Electrochem. Soc.* **2005**, 152(2), G115-G121.
11. Yeung, Ho; Chan, H.; Zou, S.; Weaver, M. J.; *J. Phys. Chem. B*. **1999**, 103, 11141-11151.

12. Josell, D.; Bonevich, J. E.; Moffat, T. P.; Aaltonen, T.; Ritala, M.; Lekela, M. *Electrochemical and Solid-State Letters*. **2006**, 9(2), C48-C50.

13. Josell, D.; Witt, C.; Moffat, T. P. *Electrochemical and Solid-State Letters*. **2006**, 9(2), C41-C43.

CHAPTER 3

THE EFFECT OF GALLIC ACID ON ACID ON CU/RU BIMETALLIC CORROSION

3.1 Introduction

Chemical mechanical planarization (CMP) and post-CMP are the two final processes in dual damascene of fabricating multilevel metal interconnects for building integrated circuits (IC's) in semiconductor industry. CMP involves polishing and planarizing the top surface of wafer which includes different metal substrates in adjacent layers such as copper (Cu) interconnects and its diffusion barriers Ta or TaN.[1,2] As the name reveals, post-CMP is usually done after CMP to clean the surface in order to remove any organic residues and particle contaminants adsorbed on Cu surface during the CMP step. The Post-CMP cleaning is conventionally done under alkaline condition.[3,4] Gallic acid (3,4,5,-Trihydroxy benzoic acid) is one of the polyphenolic organic acids used in post-CMP cleaning solution. Gallic acid is well known as autoxidant and radical scavenger.[5,6,7] In this chapter, gallic acid is investigated for its autoxidative behavior in corrosion of Cu on ruthenium (Ru) and tantalum (Ta) substrates. Praveen et al. have previously demonstrated bimetallic corrosion of Cu/Ru and Cu/Ta and have shown that Ru enhances Cu corrosion due to its noble nature.[8] We have carried out preliminary investigation of the effect of gallic acid on Cu/Ru bimetallic corrosion and examined its likely corrosion mechanism, a mechanism has been hypothesized.

3.2 Experiment

In this chapter, the experimental methods include the optical imaging of micro corrosion pattern test which will be discussed later. Also, Ru, Cu and Ta shots were used as working

electrode for electrochemical experiments. The electrochemical techniques which are employed in this chapter are CV, Tafel plot and OCP measurements. UV-Vis spectroscopy is used for quantification of the different oxidized product of gallic acid. All of these optical imaging method, electrochemical experiments, and UV-Vis spectroscopy are carried out under different pH value conditions.

3.3 Microdot Corrosion Test Pattern in Different pH Condition

In order to monitor copper corrosion rate in test solution, a novel corrosion test method is developed at the Interfacial Electrochemistry and Material Research lab. Previously, the corrosion test pattern method developed by Praveen et al. was used to study Cu corrosion in basic ammonium citrate solution.[8] In this research, the method of Cu microdot corrosion test was used in gallic acid. Copper microdots were deposited by physical vapor deposition (PVD) on the surface of different substrates such as Ta, and Ru wafer which covered with micro dot mask. The thickness of Cu microdots is ca. 70 nm and the diameter of microdots is 120 microns. The copper micropattern was immersed in test solution and the corrosion of Cu microdots were monitored under the real-time observations of microscope imaging, see figure 3-1. From the images and in each period of time, the rate of copper corrosion can be estimated in unit of nm thickness per minutes (nm/min). The advantages of using optical imaging of micropattern corrosion test are as followed: rapid corrosion monitoring, suitable for the study bimetallic contacts, estimated of corrosion rates, and understanding the effect of chemical environments.

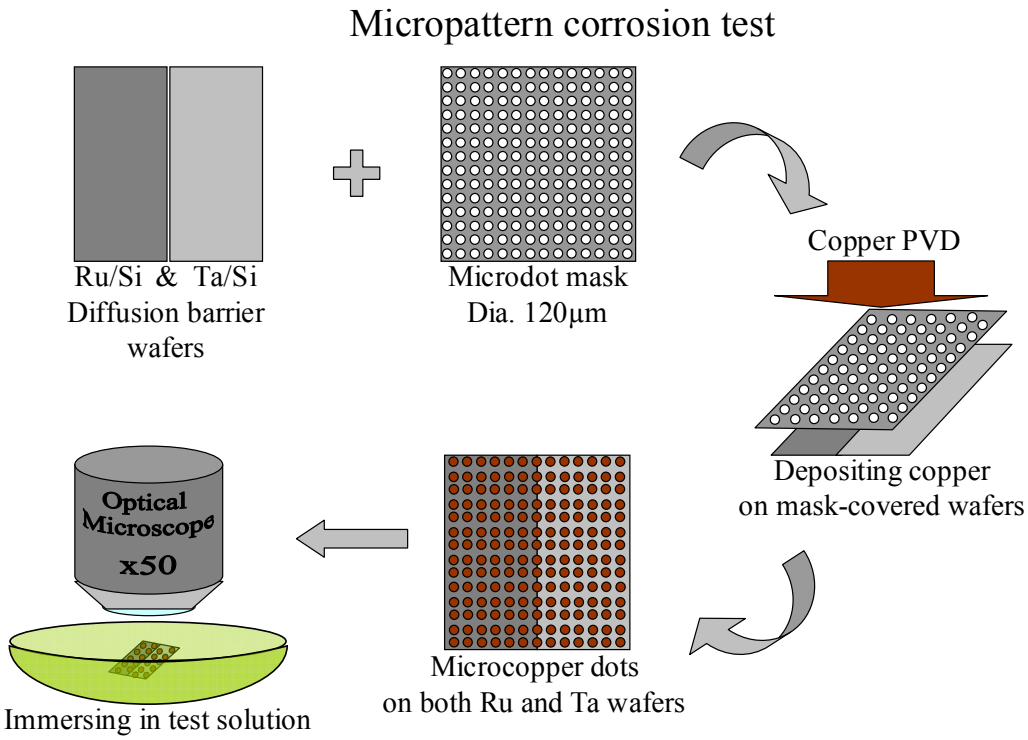

Figure 3-1: Processes of optical imaging micropattern corrosion test

In figure 3-2, the micro Cu pattern on tantalum (Ta) and ruthenium (Ru) were observed under the microscope and recorded in three pH conditions (pH 5, 9 and 12). In pH 5 the Cu dots on Ru was passivated whereas Cu on Ta still remained in metallic color. The corrosion occurred only in low alkaline condition around pH 9. The estimated corrosion rate (nm/min) in pH 9 for Cu on Ru and Ta was 3.2 nm/min and 1.7 nm/min respectively. The Cu dots on Ru corroded fast than Ta because of bimetallic corrosion which will be discussed later in the section of electrochemical measurements. In pH 12 condition, Cu on both Ru and Ta was not corroded. Ruthenium has a tendency to reduce oxygen giving hydroxyl ions in the low acidic conditions commonly referred as the oxygen reduction reaction (ORR). To explore the effect of ORR on corrosion[8], the testing environment was controlled in nitrogen saturated ambient to minimize the

effect of ORR in pH 9 gallic acid. As expected, the Cu wasn't corroded in nitrogen saturated ambient. Its worth to mention that gallic acid can form different oxidized products depending on the pH conditions. Thus purging nitrogen also inhibits the oxidation of gallic acid[9]. So, corrosion of Cu in gallic acid depends on pH, oxygen and substrate.

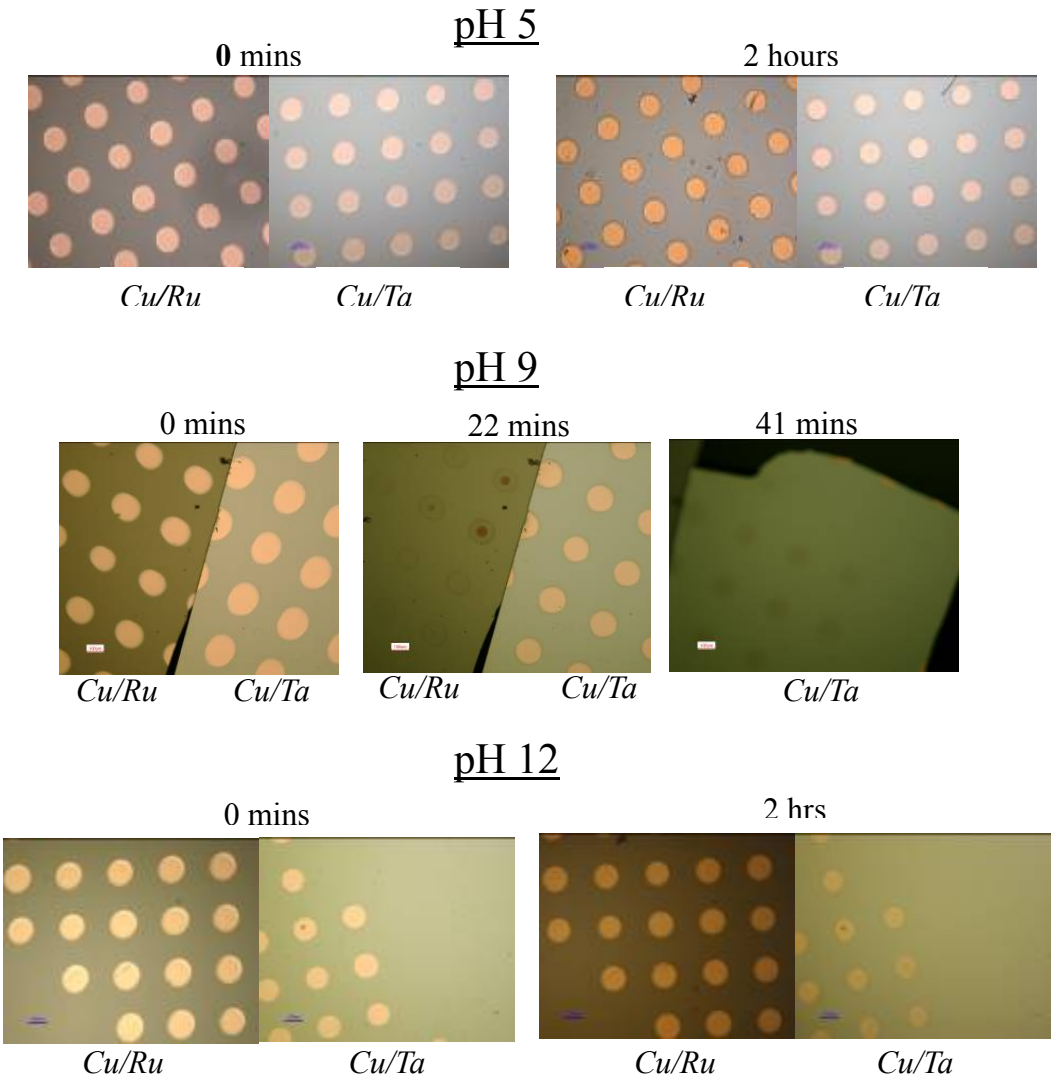

Figure 3-2: Optical images of thick Cu microdots on Ru and Ta immersed in 5 mM Gallic acid at different pH conditions. Cu dots were corroded in pH 9 in 22 minute, but Cu dots were not corroded in both pH 5 and pH 9.

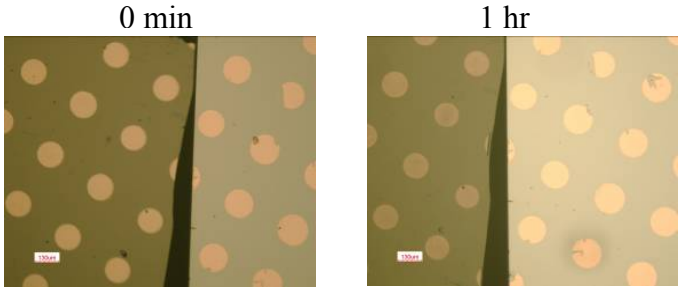

Figure 3-3 Optical images of Cu microdots on Ru and Ta immersed in 5 mM Gallic acid at pH 9 nitrogen saturated conditions. The copper dots were not corroded in 1 hour.

3.4 Oxidation of Gallic Acid by Using UV-Vis Spectroscopy in Alkaline Condition

It has been reported that gallic acid undergoes oxidation to form semi-quinone and eventually leading to quinone formation in alkaline solution (Eqn. 3-1). Another literature has reported the formation of dimer during the oxidation step at the higher pH condition. Different oxidized products can also be visually observed. Solutions prepared at 7 < pH < 11 were always green in color. However at pH 12, the solution acquired deep orange-brown color. The UV-Vis spectroscopy was used to figure out the different oxidized products of gallic acid under different pH alkaline solution.

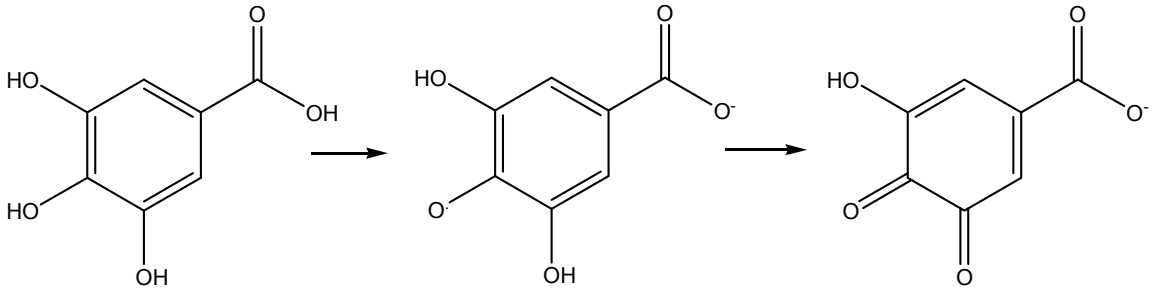

Gallic Acid Semiquinone Radical Quinone

----------Eqn. 3-1

3.4.1 UV-Visible Spectra of pH Dependent

A 5 mM gallic acid aqueous solution slowly changed its color from clear to light yellow

when exposed to air for weeks. The pH of freshly prepared 5 mM gallic acid was 3.14. Gallic acid reduced oxygen and oxidized itself due to its antioxidant behavior. The speed of its oxidation reaction depends on the pH value because the color changed more quickly when adding KOH to increase the pH value. The color changed form clear to orange, green, dark green, dark brown, which represents the different states of oxidized of gallic acid which formed the quinone or semi-quinone species. Quinone species has absorption ca. 400 nm.[10,11] In figure 3-4, the UV-Vis spectra show the formation of quinone in freshly prepared gallic acid at different pH alkaline condition. The quinone started to form around pH 6.7.

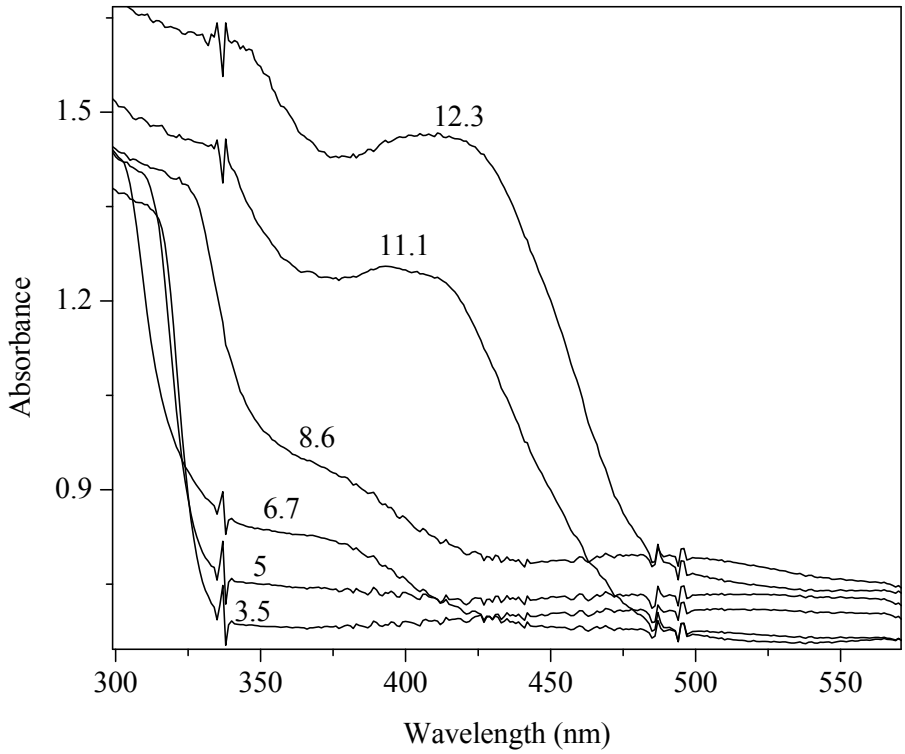

Figure 3-4: UV Vis spectra of 5 mM gallic acid at different pH conditions. Quinone starts forming around pH 6.7

3.4.2 Time Dependent UV-Vis Spectra of Gallic Acid

From the figure 3-4, gallic acid seems to form quinone easily at high alkaline condition because the colorful quinone can be quickly observed at high pH value condition. In order to evaluate the formation rate of quinone, 5 mM gallic acid was prepared in four different pH conditions which were pH 5, 6, 9, and 12. The spectrum was taken in different time interval of air exposure to determine the rate of formation of quinone. In figure 3-5, there was no quinone peak at acidic condition pH 5, whereas it grew fast at pH 9 & 12 condition. Also one can observe the difference in spectra obtained at pH 9 and 12. Insert in the figure 3-5 (d) is the comparison of gallic acid at pH 12 with ellagic acid. Similarity of spectra feature near 500 nm show the systematic formation of ellagic acid dimer (Eqn. 3-2) during oxidation of gallic acid at high pH as suggested in the literature[12].

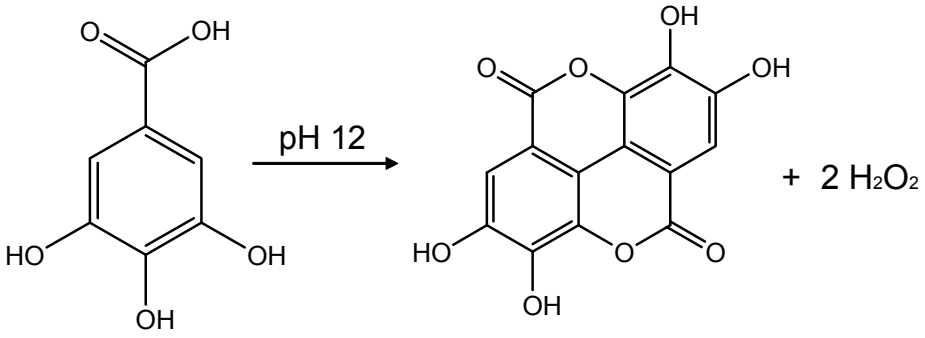

Gallic Acid Ellagic acid

----------Eqn. 3-2

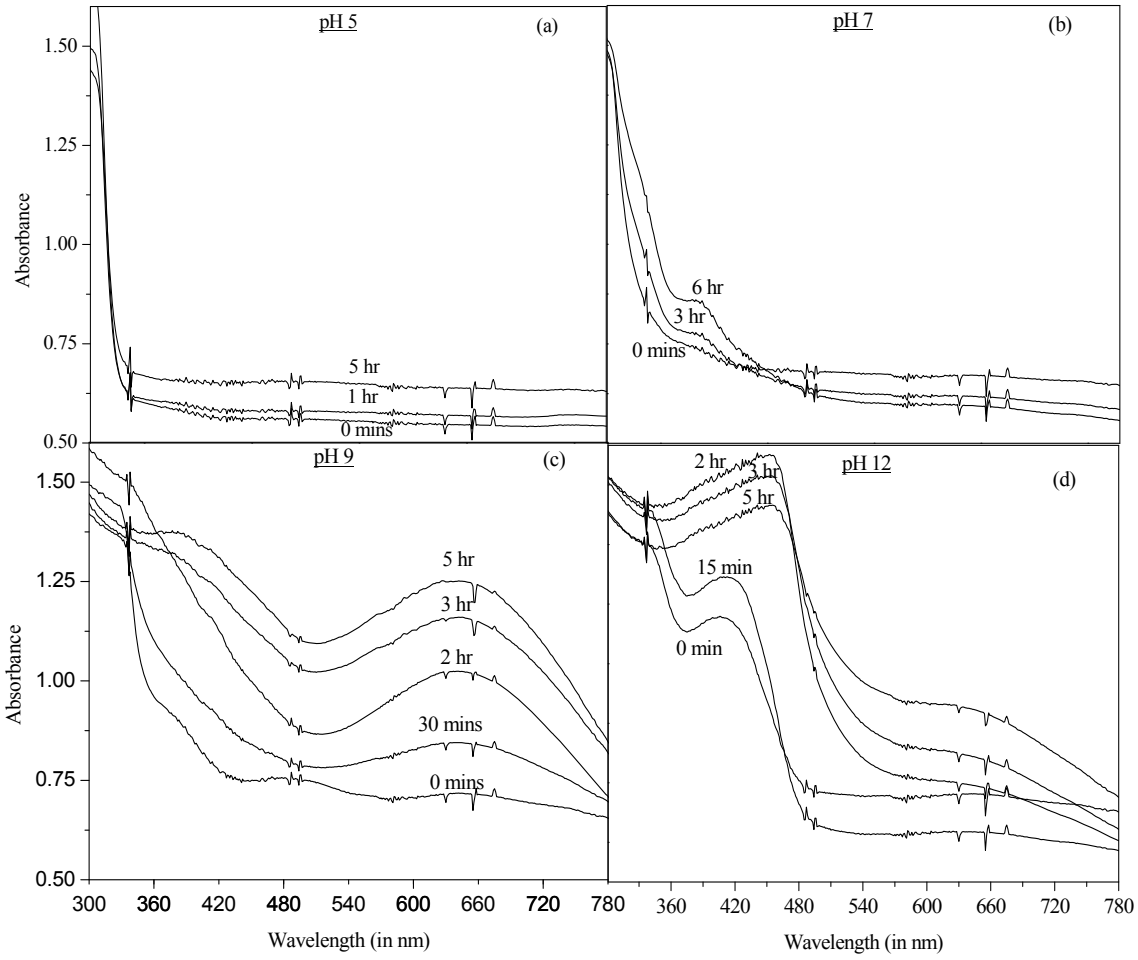

Figure 3-5: UV-Vis spectra's of 5 mM Gallic acid taken at different time intervals to study the extent of gallic acid oxidation.

3.5 Electrochemical Measurements

Cu corrosion behavior in gallic acid is dependent on pH value as demonstrated in corrosion test pattern. In order to understand the corrosion behavior, electrochemical techniques like tafel plots, CV and direct current measurement were used to illustrate the corrosion mechanism and to corroborate with the micro corrosion test pattern results.

3.5.1 Tafel Plot Measurements

Before the tafel plot measurements, the gallic acid solution was prepared in different pH (3, 6, 7.5, 9, 10, 11, and 12) condition with purging air or N_2 for 30 minutes, and the working electrode was freshly polished. The corrosion potential, E_{corr}, was collected from tafel plots in figure 3-6. Our data show that the E_{corr} of both Cu and Ru will change with increasing the pH value in nitrogen and oxygen ambient. In bimetallic corrosion system, ΔE_{corr} can be used to gauge the tendency of corrosion. Due to the cathodic protection, the preferred corrosion occurred at galvanic or sacrificial anode which is the metal with lower E_{corr} potential within the bimetallic contact. However, we observed that the Cu corrosion stopped again in higher alkaline condition (pH>12) which is consistent with the corrosion potential of Ru switched to lower position than Cu. Comparing with alkaline condition, ΔE_{corr} is large between Cu and Ru in acidic condition. Even the large ΔE_{corr}, Cu was not corroded away due to the passivation of Cu, which formed the protection layer on the top of Cu to prevent further inner corrosion. Both E_{corr} of Ru and Cu dropped when pH value of gallic acid solution was increased due to the less O_2 in gallic acid solution because the oxidation of gallic acid scavenged O_2 in alkaline condition. Hence, Ru and Cu had less chance to react with O_2 especially at high pH condition because the formation of ellagic acid dimer scavenged more O_2 in the solution. Therefore, the Cu corrosion occurred in a specific alkaline pH window in gallic acid solution, that unique feature is interesting for further study.

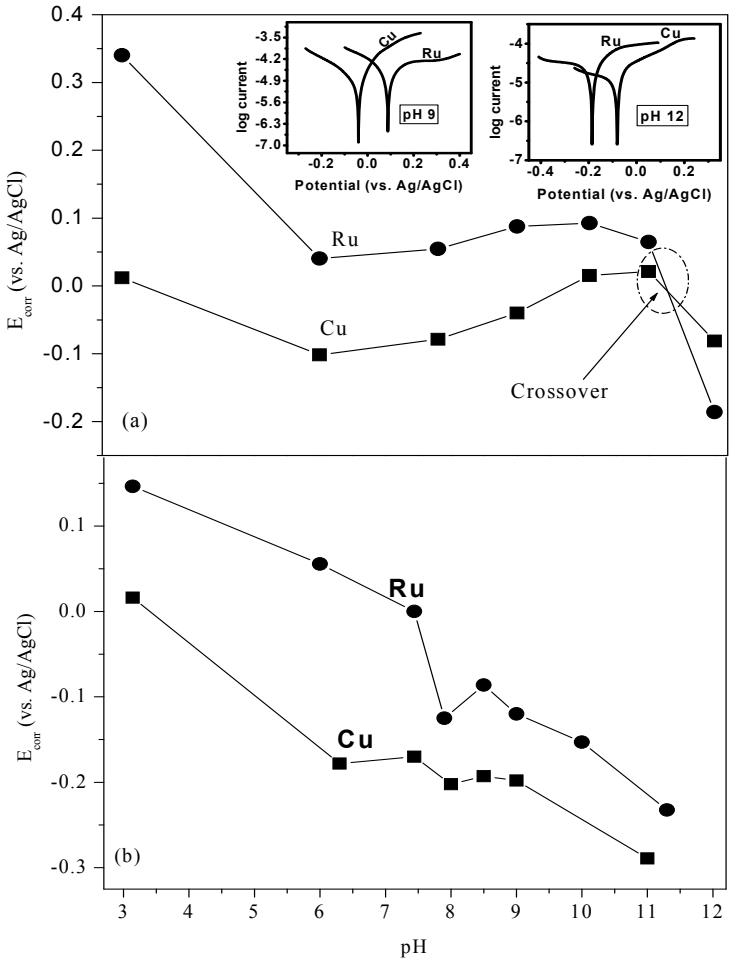

Figure 3-6: Corrosion potentials obtained from Tafel plots of Cu and Ru in (a) O_2 and (b) N_2 purged 5 mM GaAc solution. *Insert:* Tafel plots of Cu and Ru in pH 9 and 12 gallic acid solution.

3.5.2 Cyclic Voltammetry

In figure 3-7 shows CVs of Ru shot in different pH condition of 5 mM gallic acid. From those CVs, the on sets of oxidative potential of gallic acid decrease when the pH of solution increases. In other words, gallic acid oxidized more easily in high pH condition. Also, from those CVs we can conclude that the anodic current of gallic acid oxidation in high pH alkaline condition was increasing faster and higher than in low pH acidic condition. This is reason why the gallic acid is used as antioxidant in high pH alkaline condition and it is quite stable in acidic

condition. The complete CV scan also shows that the gallic acid doesn't have reduction peak in cathodic wave. That means the quinone specie which was formed from oxidizing gallic acid was irreversible.

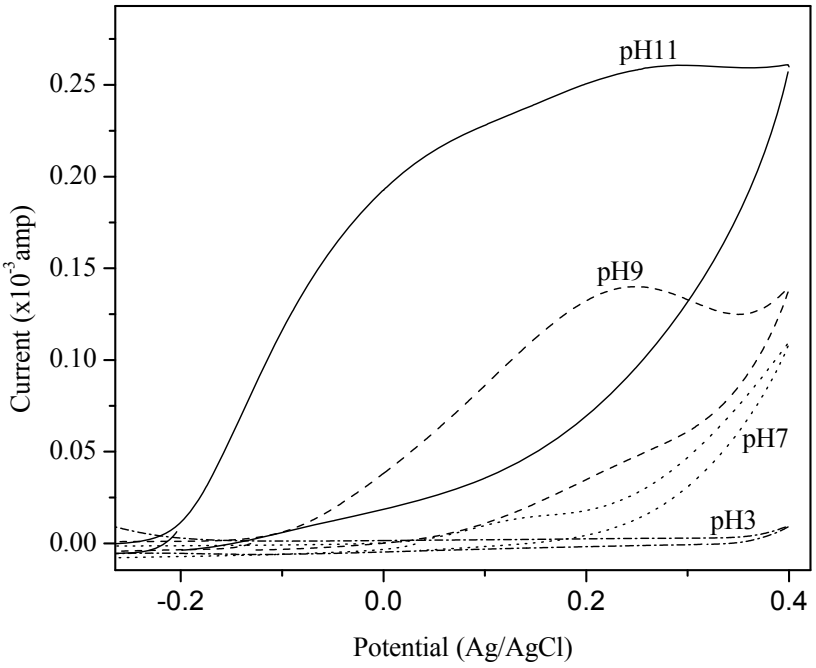

Figure 3-7: CV of 5 mM gallic acid in different pH condition

3.5.3 Direct Current Measurement

Direct current measurement in figure 3-8 was used to measure the current flow between two metals under electrical contact in solution. Two electrodes were immersed in gallic acid solution and electrically connected to Keithley 2400 source meter (Keithley Instruments Inc., Cleveland, OH). This measurement can provide information about which metal functions as cathode in the gallic acid solution. In Cu-Ta bimetallic system, the Cu is nobler than Ta, hence Ta lost electrons to form Ta oxide layer and cover on the surface, whereas Cu corroded in Cu-Ru system because Cu played as a cathode to lose electrons in pH 5 and pH 9 alkaline conditions.

However, in pH 12 the current flow switched to opposite direction comparing with lower pH condition. This is why Cu dots didn't corrode even after couple of hours in micro pattern corrosion test in pH 12. In Cu-Ta bimetallic system, the current flow from Ta to Cu was less than Cu-Ru system and current flow of Cu-Ta reached a stable state, which suggests the passivation of Cu.

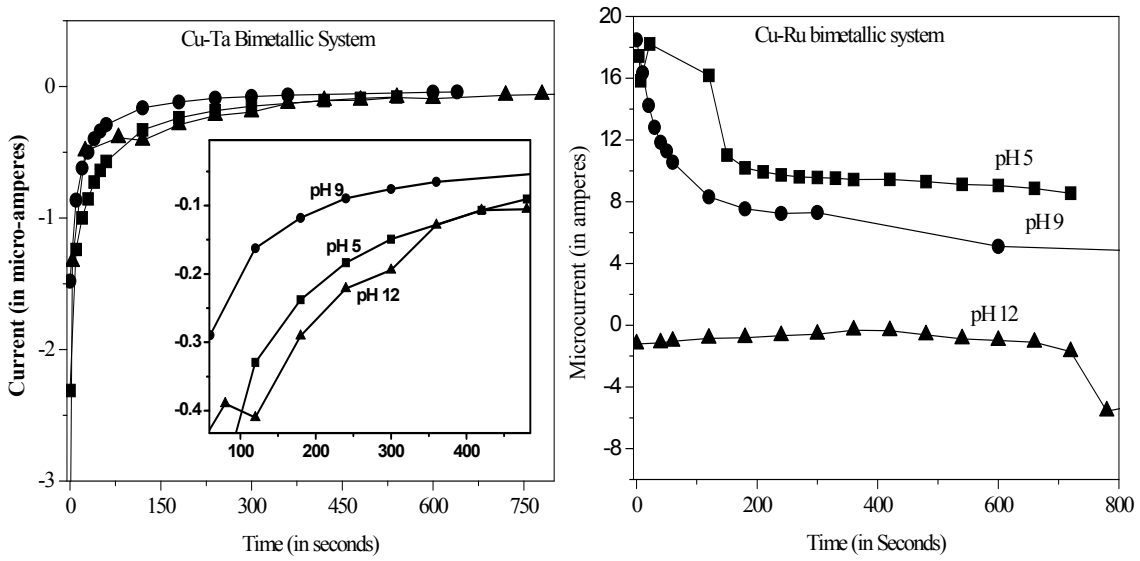

Figure 3-8: Direct current measurements of (a) Cu-Ta and (b) Cu-Ru bimetallic systems

3.6 Hypothesis and Future Work

Our experimental data have shown that bimetallic corrosion of Cu/Ta and Cu/Ru, Cu corrosion can occur when immersed in a gallic acid solution of pH around 9. The antioxidant behavior of gallic acid that associated with oxygen in the lab atmosphere likely plays a key role in the bimetallic corrosion. Also, the literatures report that oxidation of gallic acid generates hydrogen peroxide, which might cause the oxidation of Cu and influence the mechanism of Cu corrosion. In addition, it is well known that catechols and dihydroxybenzoic acids (DHBA) can chelate with metal ions to form stable metalcomplex.[13-15] The gallic acid has similar structure to

DHBA except one more hydroxyl group, so that the chelating ability to Cu could also play an important role of corrosion. Hence, further investigation of complex formation and chelating ability of gallic acid with different concentration of Cu ions are still needed in order to understanding the corrosion mechanism of Cu under bimetallic contacts in gallic acid slurry solution.

3.7 References

1. Wang, M.T.; Lin, Y. C.; & M. C. Chen. *J. Electrochem. Soc.* **1998**, 145, 7, pp 2538-2545.
2. Holloway, Karen; Foyer, Peter M. *Appl. Phys. Lett*. **1990,** 57 (17), 1736-1738.
3. Steigerwald, Joseph M.; Murarka, Shyam P.; Gutmann, Tonald J. *Chemical Mechanical Planarization of Microelectronic Materials*, John Wiley & Sons, Inc. 1997.
4. Watts, David K.; Chikamori, Yusuke; Kohama, Tatsuya; Kimura, Norio; Mishima, Koji; and Akihisa Hongo *Mat. Res. Soc. Symp. Proc.* **2001**, 671, M3.1.1-M3.1.8
5. Tambol, Chandrakant; Gautam, Banerjee *Postchemical mechanical planarization cleaning compositions*. Eur. Pat. 2005, EP 1577934
6. Naghshineh, Shahriar; Barnes, Jeff; Oldak, Ewa B: *Alkaine post chemical mechanical planarization (CMP) cleaning composition*; (ESC, Inc, USA Advanced technology materials, Inc.) US. Pat. Appl. Publ. (2001)
7. Hotta, Hiroki; Nagamo, Satomi; Ueda, Masashi; Tsujino, Yoshio; Koyama, Junko Koyama; Osakai, Toshiyuki *Biochimi. Biophys. Acta* **2002,** 1572, 123-132
8. Nalla, Praveen R.; and Chyan, Oliver; *Techcon 2005: Session 4 – IPS:* Cu Low-k/Novel interconnects, Oct 24
9. Tulyathan, Vanna; Boulton, Roger B.; Singleton, Vernon L. *J. Agric. Food Chem.* **1989**,

37, 4, 844-849.

10. Friedman, Mendel; Jürgens, Hella S. *J. Agric. Food Chem*. **2000**, 48, 2101-2110.

11. Fink, David W.; Stong, John D. *Spectrochimica acta*. **1982**, 38A, 12, 1295-1298.

12. Kiss, Tamas; Kozlowski, HenryK; Micera, Giovanni; Erre, Liliana Strinna. *Cupric ion binding by dihydroxybenzoic acids*, Polyhedron **1999**, 8(5), 647-651

13. Cariati, F.; Deiana, S.; Erre, Li; Micera, G.; Piu, P. *Inorganica Chimica Acta.* **1982**, 64, L213-L215.

14. Gerega, Krystyna; Kozlowski, Henry; Kiss, Tamas; Micera, Giovanni; Erre, Liliana Strinna; Caritati,Franco. *Inorganica Chimica Acta.* **1987**, 138, 31-34.

REFERENCES LIST

Cariati, F.; Deiana, S.; Erre, Li; Micera, G.; Piu, P. *Inorganica Chimica Acta.* **1982**, 64, L213-L215.

Chan, R.; Arunagiri, T. N.; Zhang, Y., Chyan, O.; Wallace, R. M.; Kim, M. J.; Hurd, T. Q. *Electrochemical and Solid-State Letters.* **2004**, 7(8), G154-157.

Faulkner, Larry R. *Journal of Chemical Education*. **1983**, 60(4), 262.

Friedman, Mendel; Jürgens, Hella S. *J. Agric. Food Chem*. **2000**, 48, 2101-2110.

Fink, David W.; Stong, John D. *Spectrochimica Acta*. **1982**, 38A, 12, pp 1295-1298.

Gerega, Krystyna; Kozlowski, Henry; Kiss, Tamas; Micera, Giovanni; Erre, Liliana Strinna; Caritati,Franco. *Inorganica Chimica Acta.* **1987**, 138, 31-34.

Hotta, Hiroki; Nagamo, Satomi; Ueda, Masashi; Tsujino, Yoshio; Koyama, Junko Koyama; Osakai, Toshiyuki *Biochimi. Biophys. Acta* **2002,** 1572, 123-132

Holloway, Karen; Fryer, Peter M. *Appl. Phys. Lett.* **1990**, 57(17), 22.

Josell, D.; Bonevich, J. E.; Moffat, T. P.; Aaltonen, T.; Ritala, M.; Lekela, M. *Electrochemical and Solid-State Letters*. **2006**, 9(2), C48-C50.

Josell, D.; Wheeler, D.; Witt, C.; Moffat, T. P. *Electrochemical and Solid-State Letters*. **2003**, 6(10), C143-145.

Josell, D.; Witt, C.; Moffat, T. P. *Electrochemical and Solid-State Letters*. **2006**, 9(2), C41-C43.

Kiss, Tamas; Kozlowski, HenryK; Micera, Giovanni; Erre, Liliana Strinna. *Cupric ion binding by dihydroxybenzoic acids*, Polyhedron 1999, 8(5), 647-651

Laboratory Techniques in Electroanalytical Chemistry, 2nd ed., rev. and expanded,; Kissinger, Peter T. Ed.; Heineman, William R.Ed.; Marcel Dekker, Inc.: New York, 1996; Chapter 2.

Liu, J.; Lei, J.; Magtoto, N.; Rudenja, S.; Garza, M.; Kelber, J. A. *J. Electrochem. Soc.* **2005**, 152(2), G115-G121.

Moffat, T. P.; Walker, M.; Chen, P. J.; Bonevich, J. E; Egelhoff, W. F.; Richter, L.; Witt, C.; Aaltonen, T.; Ritala, M.; Leskela, M.; Josell, D.; *J. Electrochem. Soc.* **2006**, 153(1), C37-C50.

Naghshineh, Shahriar; Barnes, Jeff; Oldak, Ewa B: *Alkaine post chemical mechanical planarization (CMP) cleaning composition*; (ESC, Inc, USA Advanced technology materials, Inc.) US. Pat. Appl. Publ. (2001)

Nalla, Praveen R.; and Chyan, Oliver; *Techcon 2005: Session 4 – IPS:* Cu Low-k/Novel interconnects, Oct 24

Olowolafe, J. O.; Mogab, C. J.; Gregory, M. Kottke. *J. Appl. Phys.* **1992**, 72(9).

Ono, H.; Nakano, T.; Ohta, T. *Appl. Phys. Lett.* **1994**, 64(12), 21.

Rao, C. N. R. *Ultra-violet and Visible spectroscopy*: Chemical applications, Plenum Press, 1967.

Rieger, Philip H. *Electrochemistry*; Chapman & Hall: New York, 1994; Chapter 1. p 3.

Schaller, R. R.: *Spectrum, IEEE*. **1997**, 34(6), 52-59.

Skoog; West; Holler; *Fundamentals of analytical chemistry*, Eighth ed.; Thomson: Belmont, 2002; Chapter 1, p 25.

Steigerwald, Joseph M.; Murarka, Shyam P.; Gutmann, Tonald J. *Chemical Mechanical Planarization of Microelectronic Materials*, John Wiley & Sons, Inc. 1997.

Tambol, Chandrakant; Gautam, Banerjee *Postchemical mechanical planarization cleaning compositions*. Eur. Pat. 2005, EP 1577934

Trethewey, Kenneth R. Corrosion for student of science and engineering, Longman Scientific & Technical: New York, 1988; Chapter 4. pp 82-86.

Tulyathan, Vanna; Boulton, Roger B.; Singleton, Vernon L. *J. Agric. Food Chem.* **1989**, 37, 4, pp 844-849.

Wang, M. T.; Lin, Y. C.; Chen, M. C. *J. Electrochem. Soc.***1998**, 145, 7.

Watts, David K.; Chikamori, Yusuke; Kohama, Tatsuya; Kimura, Norio; Mishima, Koji; and Akihisa Hongo *Mat. Res. Soc. Symp. Proc.* **2001**, 671, M3.1.1-M3.1.8

Yeung, Ho; Chan, H.; Zou, S.; Weaver, M. J.; *J. Phys. Chem. B*. **1999**, 103, 11141-11151.

Zhang, Yibin; Huang, Long; Arunagiri, Tiruchirapalli N.; Ojeda, Oscar; Flores, Sarah; Chyan, Oliver; Wallace, Robert M. *Electrochemical and Solid-State Letters.* **2004**, 7(9), C107-C110.